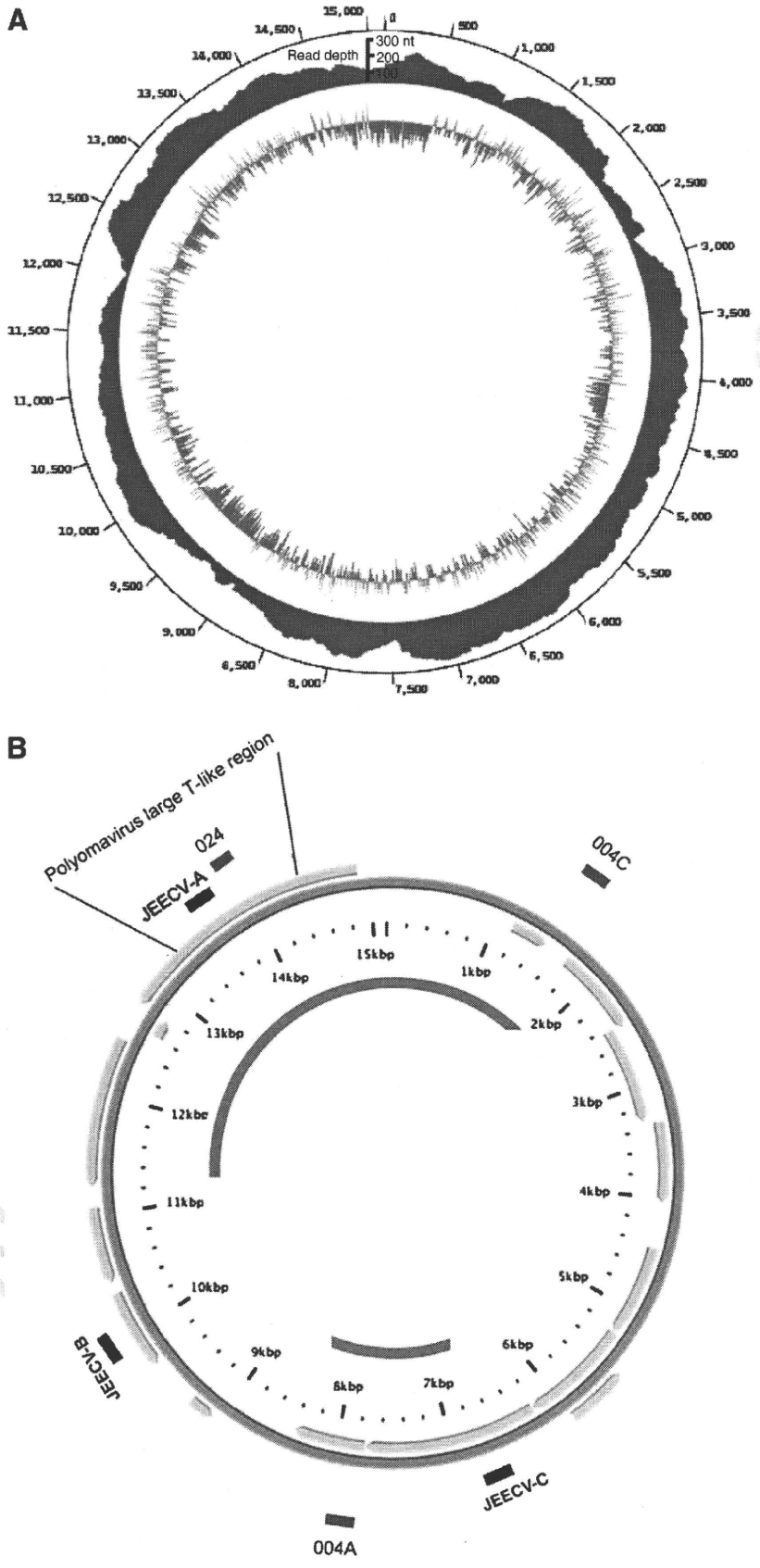

Fig. 3. Organization of the viral genome. (A) The cover depth of nucleotides analyzed using the next-generation sequencer is indicated in blue outside the JEECV genome. GC content is indicated inside the JEECV genome. Red bar, more than 50% GC content in every 10 nucleotides; green bar, less than 50% GC content. (B) Fifteen predicted ORFs are indicated with arrows. Read DNA fragments obtained using RDV and genome walking DNA fragments are indicated as blue and green lines, respectively. Black lines indicate amplified regions by PCR in Fig. 7. (For interpretation of the references to color in this figure legend, the reader is referred to the web version of this article.)

Please cite this article as: Mizutani, T., et al., Novel DNA virus isolated from samples showing endothelial cell necrosis in the Japanese eel, *Anguilla japonica*, Virology (2011), doi:10.1016/j.virol.2010.12.057

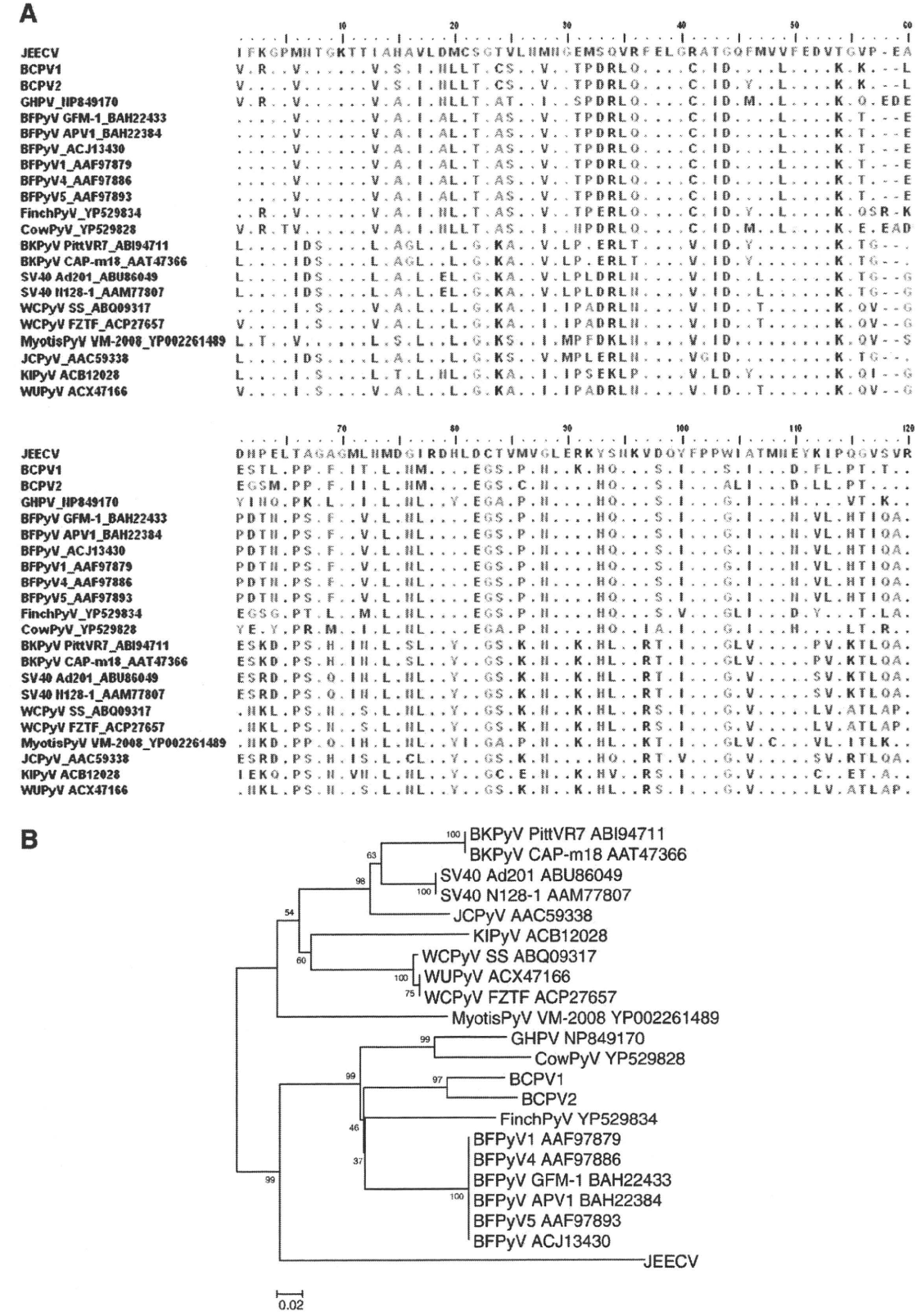

Fig. 4. Alignment of the large T-antigen-like protein. (A) Polyomavirus large T-antigen-like region of JEECV is compared with that of polyomaviruses deposited in GenBank. Alignment is performed using MEGA4 software. (B) Phylogenetic tree analysis of JEECV. The phylogenetic tree is obtained using the neighbor-joining method with 1000 bootstrap replicates, and branch length is indicated at each branch node. The horizontal scale indicates 0.02 amino acid substitutions per site. BCPV1 and 2, bandicoot papillomatosis carcinomatosis virus 1 and 2; GHPV, goose polyomavirus; BFPyV, budgerigar fledgling disease polyomavirus; finch PyV, finch polyomavirus; cow PyV, crow polyomavirus; BKPyV, BK polyomavirus; SV40, simian virus 40; WCPyV, WU polyomavirus; mytosis PyV, mytosis polyomavirus; and JCPyV, JC polyomavirus.

Please cite this article as: Mizutani, T., et al., Novel DNA virus isolated from samples showing endothelial cell necrosis in the Japanese eel, *Anguilla japonica*, Virology (2011), doi:10.1016/j.virol.2010.12.057

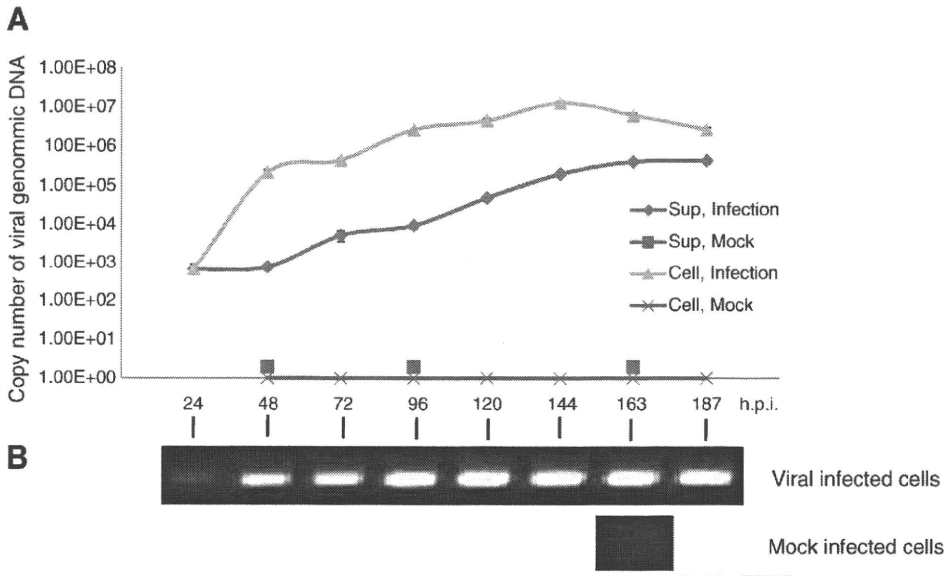

Fig. 5. Analysis of virus multiplication in JEE cells. JEECV (0.01 MOI) is infected into JEE cells. DNA extracted from cells and culture supernatant from 24 to 187 h p.i. is analyzed using real-time TaqMan PCR (A) and conventional PCR using primers, 024-3 and -4 (B).

9011R (5′-TCACTCAAGCACAGGCTATGGACCAGCCCC-3′) for 3389-bp PCR products;
8382F (5′-TCAGTCATGCCGCCTGTAGAAAGCACCTG-3′) and
12011R (5′-ACGCCCCCCATGCCTGACCCTATGTTCGG-3′) for 3629-bp PCR products;
11142F (5′-GTCATACGTCCGTGCGCTGCCCTGAGGAAC-3′) and
15011R (5′-TTTATGAAGGAAGTAATATGTGTTTAATTC-3′) for 3869-bp PCR products;
371R (5′-CAAGTATGAGTCATTTCAATTGTATGAGCC-3′) and
14442F (5′-AGTTCTGTGACCACTGATCCCAGCTTAG-3′) for 1240-bp PCR products.

Each PCR cycle consisted of 98 °C for 30 s, followed by denaturing at 98 °C for 5 s, annealing at 55 °C for 15 s, and extension at 72 °C for 15 min. This reaction was performed for 35 cycles. The nucleic acid sequences were confirmed by direct sequencing.

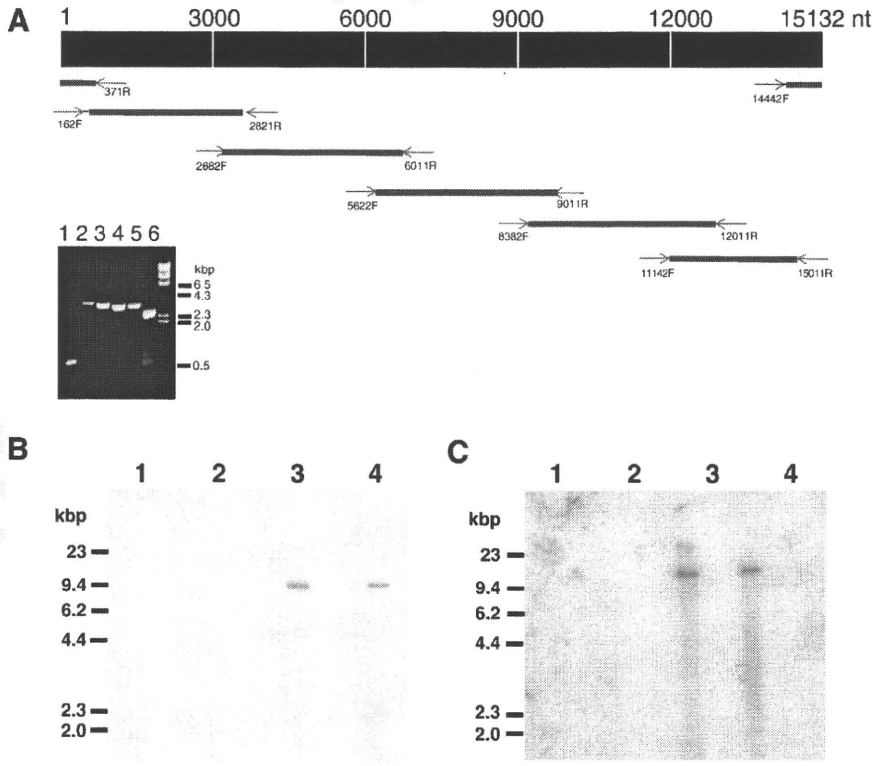

Fig. 6. Circular form of JEECV. (A) Overlapping PCR. Lane 1, 14442F and 371R primers; lane 2, 11142F and 15011R primers; lane 3, 8382F and 12011R; lane 4, 5622F and 9011R primers; lane 5, 2682F and 6011R primers; lane 6, 162F and 2821R primers. (B) Southern blot analysis with short exposure of X-ray film. (C) Southern blot analysis with long exposure using Image analyzer. Lane 1, no digested DNA from mock-infected cells; lane 2, BglII-digested DNA from mock-infected cells; and lane 3, no digested DNA from JJECV-infected cells; lane 4, BglII-digested DNA from JEECV-infected cells.

Please cite this article as: Mizutani, T., et al., Novel DNA virus isolated from samples showing endothelial cell necrosis in the Japanese eel, *Anguilla japonica*, Virology (2011), doi:10.1016/j.virol.2010.12.057

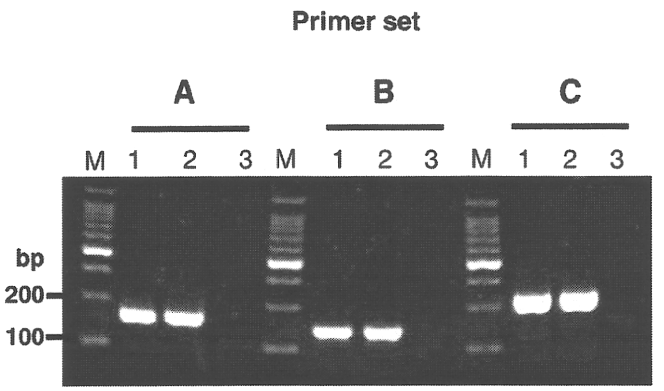

Fig. 7. Detection of JEECV in eels. Healthy eels are inoculated intraperitoneally with 1×10^6 $TCID_{50}$/cell MOI of JEECV. At 10 days p.i., DNA is extracted from gills. DNA is also extracted from gills of eel with natural VECNE and healthy eel. Conventional PCR is performed using three different primers (primer set A: JEECV-A1 and -A2, set B: JEECV-B1 and -B2, set C: JEECV-C1 and -C2). M, 100-bp DNA ladder marker; lane 1, eels with natural VECNE; lane 2, JEECV-infected eels; and lane 3, healthy eel.

For PCR with high sensitivity, we used AmpliTaq Gold Master (Applied Biosystems). The reaction mixture contained 1× master mix, 0.5 µl each of 50-µM forward and reverse primers, and template DNA. Primers are as follows (Fig. 3B):

JEECV-A1 (5′-GACGGTCCTAAACATGAACGGTGAAATGTC-3′) and JEECV-A2 (5′-GGTATTTTGTACTCATTCATAGTGGCAATC-3′) for 270 bp as primer set A;
JEECV-B1 (5′-TGGGTGACCCCGAAGGGGCACTGTACG-3′) and JEECV-B2 (5′-TATGTATAAACAGATTACGTGGCATACCTG-3′) for 240 bp as primer set B; and
JEECV-C1 (5′-TGCGCCCAGGCTTACCCTGTGCTCGATGTC-3′) and JEECV-C2 (5′-CGGGCAGACGCAGACAACGCACTGCTGAAC-3′) for 330 bp as primer set C.

Each PCR cycle consisted of activation of Taq polymerase at 95 °C for 9 min, followed by denaturing at 95 °C for 30 s, annealing at 65 °C for 30s, and extension at 72 °C for 1 min. This reaction was performed for 70 cycles. The nucleic acid sequences were confirmed by direct sequencing.

RT-PCR

RNA was extracted from JEECV- and mock-infected cells at 3 days p.i. using an Isogen RNA extraction kit (Nippon Gene, Japan). To eliminate viral DNA from the RNA solution, RNA was repurified using a Total RNA Isolation Mini Kit (Agilent Technologies Inc., USA). Furthermore, Turbo DNA free was used to digest DNA completely. cDNA was synthesized using Superscript III (Invitrogen, USA) with random primers. As a control, the reaction was performed without Superscript III enzyme. PCR was performed using primers 024-2 and 024-5 (5′-TCAGGGTGGTCTGCTTCCGG-3′) using GoTaq (30 cycles). The size of PCR products was 503 bp.

Real-time PCR

The primers and probe were designed for a segment of the large T-antigen-like region. The primers are 025-1 (5′-TTGCCGCACC-TGCTTCAG-3′) and 025-2 (5′-CGAACACCGTAATTGGAATAAAGC-3′) for a 120-bp PCR product, and the probe is 025P (5′-FAM-ACACGC-TGCTCAAATTGCTGCTGCCT-TAMRA-3′). Serial dilution of known copies of JEECV DNA as a purified PCR product (primers 024F1 and 024R1) was used as standard DNA for real-time PCR. The TaqMan real-time PCR assay was performed in a 7500 Sequence Detection System using TaqMan Gene Expression Master Mix (Applied Biosystems) according to the instruction manual. For a time-course study of viral infection, DNA was extracted from the cells and supernatant using a QIAamp DNA mini kit. Three microliters of eluted DNA (total 50 µl) from supernatant and 10-ng eluted DNA from cells were used as templates. The thermal cycling profile of this assay comprised the following steps: 2 min at 50 °C, 10 min at 95 °C, followed by 45 cycles of PCR at 95 °C with denaturing for 15 s and at 60 °C for 1 min with annealing/extension for 1 min. The TaqMan assay was performed triplicate for each sample. DNA standards (copy number: 1 to 1×10^7) were used to construct a standard curve.

Southern blot analysis

Frozen cell pellets of virus-infected and uninfected cells were thawed and resuspended in 200-µl PBS (−). The samples were then frozen and thawed two more times followed by centrifugation with 13,000*g* at 4 °C for 10 min to produce pellets. The supernatant, approximately 200 µl, was extracted for DNA using the QIAamp MiniElute virus spin kit (Qiagen), and the extracted DNA was resuspended in 100 µl of buffer AVE. DNA (1.7 µg) was digested using BglII for 4 h or not digested and run in 0.8% agarose gels. The probe used was the gel-purified PCR product using 2682F and 6011R primers, and the Megaprime DNA Labeling System (GE Healthcare) was used for ^{32}P-labeling. Hybridization was performed in ULTRAhyb (Ambion) with labeled probe at 42 °C for 15 h. Membrane washing was performed six times under the condition of 0.1× SSC and 0.1% SDS at 42 °C for 15 min. The signal was detected using X-ray film and Image analyzer (FLA2000, Fuji film, Japan).

Analysis using next generation sequencer

Viral DNA was extracted using a QIAamp DNA mini kit after precipitation using ultracentrifugation of 30-ml virus-infected supernatant (T-75 flask; Falcon) at 4 days p.i. The viral DNA was randomly amplified using Genomiphi V2 (GE Healthcare, USA) containing Phi29 enzyme, and single-stranded DNA was digested using S1 nuclease. The Genome Sequencer FLX System (Roche and 454 Life Sciences) was used in this study. DNA sequencing libraries were constructed and sequenced using Hokkaido System Science Ltd. The total number of reads was 17,000, and the total number of bases was 5,146,764. The read sequences were analyzed using GS *De novo* Assembler Version 2.3 (Roche) for *de novo* assembly.

Alignment of amino acid sequences

Nucleic acid sequences of JEECV were analyzed using BLASTx at NCBI. The polyomavirus large T-antigen-like region of JEECV was compared with that of polyomaviruses deposited in GenBank. Alignment was performed using MEGA4 software.

Acknowledgments

We thank Ms. Momoko Ogata of the National Institute of Infectious Diseases of Japan for her assistance. This study was supported in part by a grant from the Ministry of Education, Culture, Sports, Science, and Technology, Japan (#21580235 Scientific Research C:general).

References

Bennett, M.D., Woolford, L., Stevens, H., Van Ranst, M., Oldfield, T., Slaven, M., O'Hara, A.J., Warren, K.S., Nicholls, P.K., 2008. Genomic characterization of a novel virus found in papillomatous lesions from a southern brown bandicoot (Isoodon obesulus) in Western Australia. Virology 376, 173–182.

Bennett, M.D., Reiss, A., Stevens, H., Heylen, E., Van Ranst, M., Wayne, A., Slaven, M., Mills, J.N., Warren, K.S., O'Hara, A.J., Nicholls, P.K., 2010. The first complete papillomavirus genome characterized from a marsupial host: a novel isolate from *Bettongia penicillata*. J. Virol. 84, 5448–5453.

Please cite this article as: Mizutani, T., et al., Novel DNA virus isolated from samples showing endothelial cell necrosis in the Japanese eel, *Anguilla japonica*, Virology (2011), doi:10.1016/j.virol.2010.12.057

Egusa, S., Tanaka, M., Ogami, H., Oka, H., 1989. Histopathological observations on an intense congestion of the gills in cultured Japanese eel, *Anguilla japonica*. Fish Pathol. 24, 51–56.

Inoue, K., Miwa, S., Aoshima, H., Oka, H., Sorimachi, M., 1994. A histopathological study on the etiology of intense congestion of the gills of Japanese eel, *Anguilla japonica*. Fish Pathol. 29, 35–41.

John, R., Muller, H., 2007. Polyomaviruses of birds: etiologic agents of inflammatory diseases in a tumor virus family. J. Virol. 81, 11554–11559.

Maeda, K., Hondo, E., Terakawa, J., Kiso, Y., Nakaichi, M., Endoh, D., Sakai, K., Morikawa, S., Mizutani, T., 2008. Isolation of a novel adenovirus from a fruit bat (*Pteropus dasymallus yayeyamae*). Emerg. Infec. Dis. 14, 347–349.

Mizutani, T., Endoh, D., Okamoto, M., Shirato, K., Shimizu, H., Arita, M., Fukushi, S., Saijo, M., Sakai, K., Limn, C.K., Ito, M., Nerome, R., Takasaki, T., Ishii, K., Suzuki, T., Kurane, I., Morikawa, S., Nishimura, H., 2007. Rapid genome sequencing of RNA viruses. Emerg. Infec. Dis. 13, 322–324.

Ono, S., Nagai, A., 1997. Electronmicroscopic observation and experimental infection of congestion in gills of Japanese eel, *Anguilla japonica*. J. School Marine Sci. Technol. 43, 95–105.

Ono, S., Wakabayashi, K., Nagai, A., 2007. Isolation of the virus causing viral endothelial cell necrosis of eel from cultured Japanese eel, *Anguilla japonica*. Fish Pathol. 42, 191–200.

Pipas, J.M., 1992. Common and unique features of T antigens encoded by the polyomavirus group. J. Virol. 66, 3979–3985.

Sakai, K., Ueno, Y., Ueda, S., Yada, K., Fukushi, S., Saijo, M., Kurane, I., Mutoh, K., Yoshioka, K., Nakamura, M., Takehara, K., Morikawa, S., Mizutani, T., 2009. Novel reovirus isolation from an Ostrich (*Struthio camelus*) in Japan. Vet. Microbiol. 134, 227–232.

Tanaka, M., Satoh, T., Ma, W.J., Ono, S., 2008. Effectiveness of increasing temperature of rearing water and non-feeding against viral endothelial cell necrosis of eel. Fish Pathol. 43, 79–82.

Watanabe, S., Maeda, K., Suzuki, K., Ueda, N., Iha, K., Taniguchi, S., Shimoda, H., Kato, K., Yoshikawa, Y., Morikawa, S., Kurane, I., Akashi, H., (in press). Identification of a novel betaherpesvirus in bats using a rapid determination system for viral RNA sequences (RDV). Emerg. Infect. Dis.

Watanabe, S., Ueda, N., Iha, K., Masangkay, J.S., Fujii, H., Alviola, P., Mizutani, T., Maeda, K., Yamane, D., Walid, A., Kato, K., Kyuwa, S., Tohya, Y., Yoshikawa, Y., Akashi, H., 2009. Detection of a new bat gammaherpesvirus in the Philippines. Virus Genes 39, 90–93.

Woolford, L., Rector, A., Van Ranst, M., Ducki, A., Bennett, M.D., Nicholls, P.K., Warren, K. S., Swan, R.A., Wilcox, G.E., O'Hara, A.J., 2007. A novel virus detected in papillomas and carcinomas of the endangered western barred bandicoot (*Perameles bougainville*) exhibits genomic features of both the Papillomaviridae and Polyomaviridae. J. Virol. 81, 13280–13290.

Woolford, L., O'Hara, A.J., Bennett, M.D., Slaven, M., Swan, R., Friend, J.A., Ducki, A., Sims, C., Hill, S., Nicholls, P.K., Warren, K.S., 2008. Cutaneous papillomatosis and carcinomatosis in the Western barred bandicoot (*Perameles bougainville*). Vet. Pathol. 45, 95–103.

Woolford, L., Bennett, M.D., Sims, C., Thomas, N., Friend, J.A., Nicholls, P.K., Warren, K.S., O'Hara, A.J., 2009. Prevalence, emergence, and factors associated with a viral papillomatosis and carcinomatosis syndrome in wild, reintroduced, and captive western barred bandicoots (*Perameles bougainville*). EcoHealth 6, 414–425.

Yamao, T., Eshita, Y., Kihara, Y., Satho, T., Kuroda, M., Sekizuka, T., Nishimura, M., Sakai, K., Watanabe, S., Akashi, H., Rongsriyam, Y., Komalamisra, N., Srisawat, R., Miyata, T., Sakata, A., Hosokawa, M., Nakashima, M., Kashige, N., Miake, F., Fukushi, S., Nakauchi, M., Saijo, M., Kurane, I., Morikawa, S., Mizutani, T., 2009. Novel virus discovery from field-collected mosquito larvae using an improved system for rapid determination of viral RNA sequences (RDV ver4.0). Arch. Virol. 154, 153–158.

Please cite this article as: Mizutani, T., et al., Novel DNA virus isolated from samples showing endothelial cell necrosis in the Japanese eel, *Anguilla japonica*, Virology (2011), doi:10.1016/j.virol.2010.12.057

Involvement of PA28γ in the Propagation of Hepatitis C Virus

Kohji Moriishi,[1] Ikuo Shoji,[2] Yoshio Mori,[1] Ryosuke Suzuki,[3] Tetsuro Suzuki,[3] Chikako Kataoka,[1] and Yoshiharu Matsuura[1]

We have reported previously that the proteasome activator PA28γ participates not only in degradation of hepatitis C virus (HCV) core protein in the nucleus but also in the pathogenesis in transgenic mice expressing HCV core protein. However, the biological significance of PA28γ in the propagation of HCV has not been clarified. PA28γ is an activator of proteasome responsible for ubiquitin-independent degradation of substrates in the nucleus. In the present study, knockdown of PA28γ in cells preinfection or postinfection with the JFH-1 strain of HCV impaired viral particle production but exhibited no effect on viral RNA replication. The particle production of HCV in PA28γ knockdown cells was restored by the expression of an small interfering RNA (siRNA)-resistant PA28γ. Although viral proteins were detected in the cytoplasm of cells infected with HCV, suppression of PA28γ expression induced accumulation of HCV core protein in the nucleus. HCV core protein was also degraded in the cytoplasm after ubiquitination by an E3 ubiquitin ligase, E6AP. Knockdown of PA28γ enhanced ubiquitination of core protein and impaired virus production, whereas that of E6AP reduced ubiquitination of core protein and enhanced virus production. Furthermore, virus production in the PA28γ knockdown cells was restored through knockdown of E6AP or expression of the siRNA-resistant wild-type but not mutant PA28γ incapable of activating proteasome activity. *Conclusion:* Our results suggest that PA28γ participates not only in the pathogenesis but also in the propagation of HCV by regulating the degradation of the core protein in both a ubiquitin-dependent and ubiquitin-independent manner. (HEPATOLOGY 2010;52:411-420)

Over 170 million individuals worldwide are infected with hepatitis C virus (HCV), which is a major etiological agent of liver diseases, including hepatic steatosis, cirrhosis, and hepatocellular carcinoma (HCC).[1] HCV is classified into the genus Hepacivirus of the *Flaviviridae* family and has a positive, single-strand RNA genome that encodes a single polyprotein consisting of about 3,000 amino acids.[2] The N-terminal one-third of the polyprotein is occupied by the structural proteins, and the remaining portion consists of nonstructural proteins involved in viral replication and assembly. Host and viral proteases cleave the appropriate sites of the polyprotein, resulting in generation of at least 10 viral proteins. The capsid (core), E1 and E2 proteins, and p7 are cleaved off by signal peptidase from the polyprotein. Furthermore, the C-terminal signal sequence of the core protein is processed by signal peptide peptidase.[3] Our recent data indicate that signal peptide peptidase cleaves the polyprotein between Phe[177] and Leu[178] in the signal sequence, and this processing is required for HCV propagation.[4] The mature core proteins make nucleocapsid with viral RNA, and HCV particles bud into the lumen of the endoplasmic reticulum bearing E1 and E2 glycoproteins on the host lipid components, and are released from the host cells.

Several reports suggest that HCV core protein plays an important role in the development of various outcomes of liver failure, including steatosis and HCC.[5,6]

Abbreviations: HA, hemagglutinin; HCC, hepatocellular carcinoma; HCV, hepatitis C virus; JEV, Japanese encephalitis virus; moi, multiplicity of infection; shRNA, short hairpin RNA; siRNA, small interfering RNA.

From the [1]Department of Molecular Virology, Research Institute for Microbial Diseases, Osaka University, Osaka, Japan; the [2]Division of Microbiology, Kobe University Graduate School of Medicine, Hyogo, Japan; and the [3]Department of Virology II, National Institute of Infectious Diseases, Tokyo, Japan.

Received February 3, 2010; accepted March 13, 2010.

Supported in part by grants-in-aid from the Ministry of Health, Labor, and Welfare; the Ministry of Education, Culture, Sports, Science, and Technology; the Osaka University Global Center of Excellence Program; and the Foundation for Biomedical Research and Innovation.

Potential conflict of interest: Nothing to report.

Address reprint requests to: Yoshiharu Matsuura, D.V.M., Ph.D., Department of Molecular Virology, Research Institute for Microbial Diseases, Osaka University, 3-1 Yamada-oka, Suita, Osaka 565-0871, Japan. E-mail: matsuura@biken.osaka-u.ac.jp; fax: (81)-6-6879-8269.

Published online in Wiley InterScience (www.interscience.wiley.com).

DOI 10.1002/hep.23680

Additional Supporting Information may be found in the online version of this article.

We have reported previously that HCV core protein specifically interacts with a proteasome activator PA28γ/REGγ in the nucleus and is digested by a PA28γ-dependent proteasome activity.[7] *In vivo* experiments in a mouse model suggest that PA28γ plays a critical role in the pathogenesis induced by HCV core protein.[8,9] PA28γ forms a homoheptamer in the nucleus and enhances the proteasome-mediated cleavage after basic amino acid residues, whereas PA28α and PA28β exhibit 41% and 34% homology to PA28γ, respectively, and form a heteroheptamer in the cytoplasm to activate cleavage after hydrophobic, acidic, or basic amino acid residues.[10] Recently, several groups reported that PA28γ interacts with steroid receptor coactivator-3 and cell cycle suppressors such as $p21^{WAF1/CIP1}$, $p16^{INK4A}$, and $p19^{ARF}$, and enhances the degradation of these proteins in a ubiquitin- and adenosine triphosphate–independent manner.[11-13] Furthermore, other mechanisms of ubiquitin-independent degradation have been considered for cell cycle regulation, summarized in the review of Jariel -Encontre et al.[14] However, the precise physiological functions of PA28γ are largely unknown *in vivo*, because PA28γ-knockout mice exhibit only mild growth retardation and live approximately as long as their control littermates.[15,16]

HCV core protein is degraded in a PA28γ-dependent and ubiquitin-independent manner in the nucleus,[7,17] while E6AP is also involved in the degradation of the core protein in a ubiquitin-dependent manner.[17,18] E6AP is a member of E3 ligases, which catalyze ubiquitin ligation of host and foreign proteins. Knockdown of E6AP suppressed degradation of HCV core protein and enhanced the release of infectious particles, suggesting that E6AP negatively regulates HCV propagation.[18] However, the role of PA28γ in the propagation of HCV has not yet been characterized. In this study, we examined the biological significance of PA28γ in the propagation of HCV.

Materials and Methods

Transfection, Immunoblotting, and RNA Interference. Plasmid DNA was transfected into Huh7OK1 cells by way of liposome-mediated transfection using Lipofectamine LTX with Plus reagent (Invitrogen, Carlsbad, CA). Expression of HCV core protein was determined by way of enzyme-linked immunosorbent assay as described.[19] Immunoblotting was performed as described.[8] The small interfering RNAs (siRNAs) targeted to the PA28γ gene were purchased from Ambion (Austin, TX) and were introduced into the cell lines using Lipofectamine RNAiMax (Invitrogen). siRNAs with the Ambion siRNA ID numbers 138669 and 138670 were designated as siPA28γ1 and siPA28γ2, respectively. Antibodies and plasmids are described in the Supporting Information.

Cell Lines and Virus Infection. All cell lines were cultured at 37°C under the conditions of humidified atmosphere and 5% CO_2. The human hepatoma cell line Huh7OK1 and derivative cell lines were maintained in Dulbecco's modified Eagle's medium (Sigma, St. Louis, MO) supplemented with nonessential amino acids, sodium pyruvate, and 10% fetal bovine serum. The Huh7-derived cell line harboring a subgenomic or a full-length HCV replicon RNA[20] was maintained in Dulbecco's modified Eagle's medium containing 10% fetal bovine serum, nonessential amino acids, sodium pyruvate, and 1 mg/mL G418 (Nakarai Tesque, Kyoto, Japan). Huh7OK1 cells were transfected with pSilencer-shPA28γ4 or a control plasmid, pSilencer 2.1 U6 hygro negative control (Ambion), and drug-resistant clones were selected by treatment with hygromycin (Wako, Tokyo, Japan) at a final concentration of 100 μg/mL. Huh7OK1 cells transfected with the control plasmid were selected with puromycin and designated as shCntrl, whereas those transfected with pSilencer-shPA28γ4 were established by limited dilution,[8] and two of the resulting cell lines were designated as KD5 and KD7. Plasmids encoding wild-type or mutant PA28γ complementary DNAs resistant to siRNA against PA28γ were prepared by using the silent mutations as reported.[8] These plasmids were transfected into Huh7OK1 cells and cultivated in medium containing 0.1 μg/mL of puromycin for 2 days. The surviving cells were used for virus infection. The shCtrl and KD5 cells were transformed with pSilencer shE6AP or pSilencer 3.1 H1 puro negative control (Ambion) and treated with 0.1 μg/mL of puromycin for 2 days. The surviving cells were infected with JFH-1 virus at a multiplicity of infection (moi) of 0.05. The viral RNA derived from the plasmid pJFH1 was transcribed and introduced into Huh7OK1 cells according to the method of Wakita et al.[21] The infectivity of JFH1 strain was determined using a focus-forming assay[21] and is expressed in focus-forming units. The Huh7 cell line harboring subgenomic replicon RNA of the Con1 or JFH1 strain was prepared according to the method of Pietschmann et al.[22] The infectivity of the Japanese encephalitis virus (JEV) was determined by an immunostaining focus assay as described[23] and is expressed in focus-forming units. Colony formation and replication assays, quantitative

reverse-transcription polymerase chain reaction, and estimation of cell growth was performed as described in the Supporting Information.

Immunofluorescent Staining. Huh7OK1-derived cells were seeded at 0.5×10^4 cells/well in an eight-well chamber slide, infected with JFH-1 virus at an moi of 0.3 after incubation at 37°C for 24 hours, stained with Bodipy 558/568 C_{12} according to the method of Targett-Adams et al.[24] at 4 days postinfection, and then fixed at 4°C for 30 mintues with 4% paraformaldehyde in phosphate-buffered saline. After treatment of cells with 1 μg/mL of RNase A, nuclei were stained with 50 μM Heachest 33258. The fixed cells were permeabilized with 20 mM Tris-HCl containing 1% Nonidet P-40 and 135 mM NaCl at room temperature for 5 minutes, reacted with rabbit anti-core or anti-NS5A antibody followed by Alexa Fluor 488-goat antibody to rabbit immunoglobulin G, washed three times with phosphate-buffered saline, and observed with a FluoView FV1000 laser scanning confocal microscope (Olympus, Tokyo, Japan). The percentage of the area occupied by the core protein in nucleus and cytoplasm was calculated using Image-Pro software (Media Cybernetics). The percentage of the nuclear core protein to the total core protein was examined randomly in 10 fields of every three wells. The percentage of the nuclear NS5A to total NS5A was estimated by the same method as the ratio of the core protein.

Results

Transient Knockdown of PA28γ Prior to or After Infection With HCV Reduces Particle Production. We reported previously that Huh7OK1 cells are as permissive to JFH-1 virus infection as Huh7.5.1 cells.[25] The Huh-7OK1 cell line retained the ability to produce type I IFNs through the RIG-I–dependent signaling pathway upon infection with RNA viruses and exhibited a cell surface expression level of human CD81 comparable to that of the parental cell line. However, the mechanism through which the Huh7 OK1 cell line exhibits highly permissive to JFH-1 virus infection has not been clarified yet. Two siRNAs were used to knock down PA28γ, but only one, siPA28γ1, was used because the other had off-target effects (Supporting Fig. 1). To examine the effect of PA28γ on the propagation of HCV, siPA28γ1 was introduced into Huh7OK1 cells 24 hours before infection. The levels of viral RNA, core protein, and infectious viral titer were determined at 48 and 96 hours postinfection. Viral RNA in the culture supernatant and cells was clearly reduced by the knockdown of PA28γ at 48 and 96 hours postinfection, respectively (Fig. 1A), whereas a significant reduction of core protein expression was detected at 96 hours but not at 48

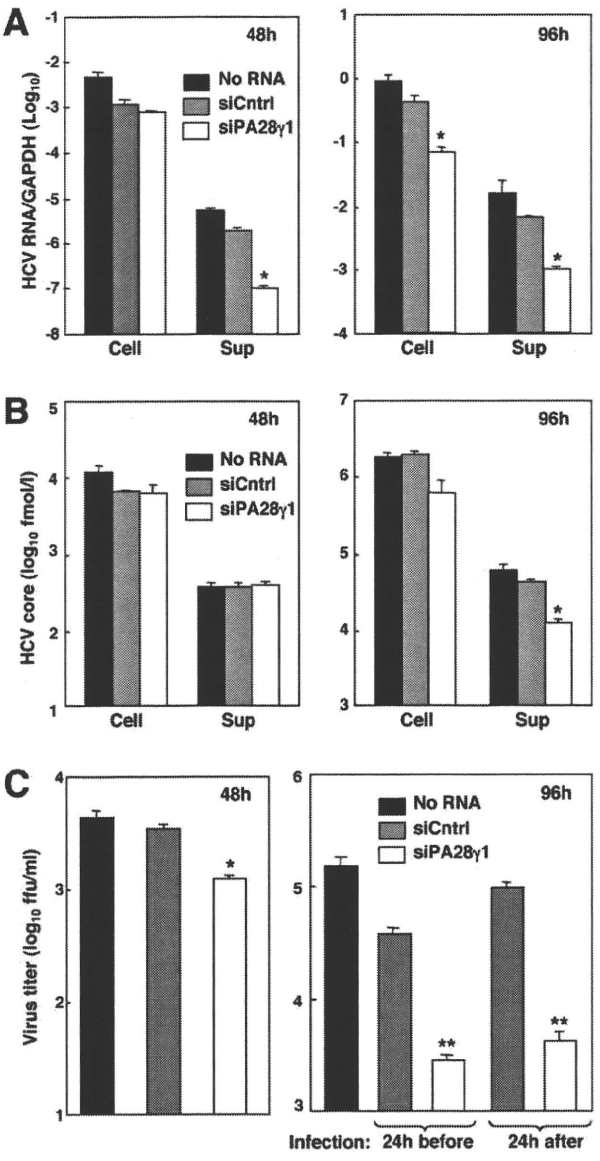

Fig. 1. Transient knockdown of PA28γ before or after infection with HCV reduces particle production. (A) Huh7OK1 cells transfected with a control siRNA (siCntrl) or PA28γ siRNA1 were infected with JFH-1 virus at 24 hours posttransfection and then harvested at 48 hours (left panel) and 96 hours postinfection (right panel). The quantity of HCV RNA in cells and supernatants was determined by way of quantitative reverse-transcription polymerase chain reaction. (B) The expression of HCV core protein in cells and supernatants at 48 hours (left panel) and 96 hours (right panel) postinfection was determined by ELISA. (C) Huh7OK1 cells that were transfected with siCntrl or PA28γ siRNA1 were infected with JFH-1 virus at 24 hours posttransfection. The infectivity of the virus in the culture supernatant was determined by a focus-forming assay at 48 hours postinfection (left panel). Those transfected with the siRNAs at 24 hours before and after infection with JFH-1 virus were determined similarly at 96 hours postinfection (right panel). $*P < 0.05$, $**P < 0.01$ versus control siRNA-transfected cells. Data are representative of three independent experiments.

hours postinfection (Fig. 1B). Infectious viral titer in the culture supernatant was significantly reduced at 48 and 96 hours postinfection by the PA28γ knockdown (Fig. 1C), consistent with the suppression of the viral RNA in the supernatant. Furthermore, a comparable suppression of the production of infectious particles in the supernatant was also achieved by introducing siPA28γ1 into cells even at 24 hours postinfection (Fig. 1C, right panel). These results suggest that PA28γ participates in the regulation of HCV propagation in postentry steps.

Stable Knockdown of PA28γ Impairs Viral Propagation. To establish the PA28γ knockdown cell lines, Huh7OK1 cells were transfected with a plasmid encoding a short hairpin RNA (shRNA) targeted to PA28γ and selected with hygromycin, resulting in two clones—KD5 and KD7—that exhibited a clear reduction of PA28γ expression (Fig. 2A). Although the suppression of PA28γ expression in KD7 cells was slightly more efficient than that in KD5 cells, the growth of KD7 cells was impaired (Fig. 2B). Viral production in the culture supernatants in cells infected with the JFH-1 virus was significantly impaired in PA28γ knockdown KD5 cells compared with control cells (Fig. 2C). The viral RNA and core protein in the supernatant were also reduced in KD5 cells (Fig. 2D). Expression of siRNA-resistant PA28γ in PA28γ knockdown KD5 and KD7 cells recovered virus production in the supernatant to a level similar to that in the control cells transfected with an empty vector, and overexpression of siRNA-resistant PA28γ in control cells slightly enhanced virus production (Fig. 2E). Our previous data suggest that capsid protein of JEV does not bind to PA28γ.[7] To examine whether PA28γ regulates JEV propagation, KD5 and shCntrl cells were infected with JEV at an moi of 0.5. The infectivity of JEV in KD5 cells was similar to that in shCntrl cells (Fig. 2F), suggesting that PA28γ does not participate in the virus production pathway of JEV. These results further support the notion that PA28γ participates in HCV propagation.

Knockdown of PA28γ Exhibits No Effect on Viral RNA Replication. Although knockdown of PA28γ resulted in the suppression of viral particle and RNA production in the culture supernatant at 48 hours postinfection with JHF-1 virus, viral RNA in the cells was not reduced (Fig. 1), suggesting that PA28γ does not participate in viral replication. To gain more insight on this point, we examined the effect of PA28γ knockdown on RNA replication in replicon cells. Transient knockdown of PA28γ through introduction of siPA28γ into the subgenomic HCV replicon cells

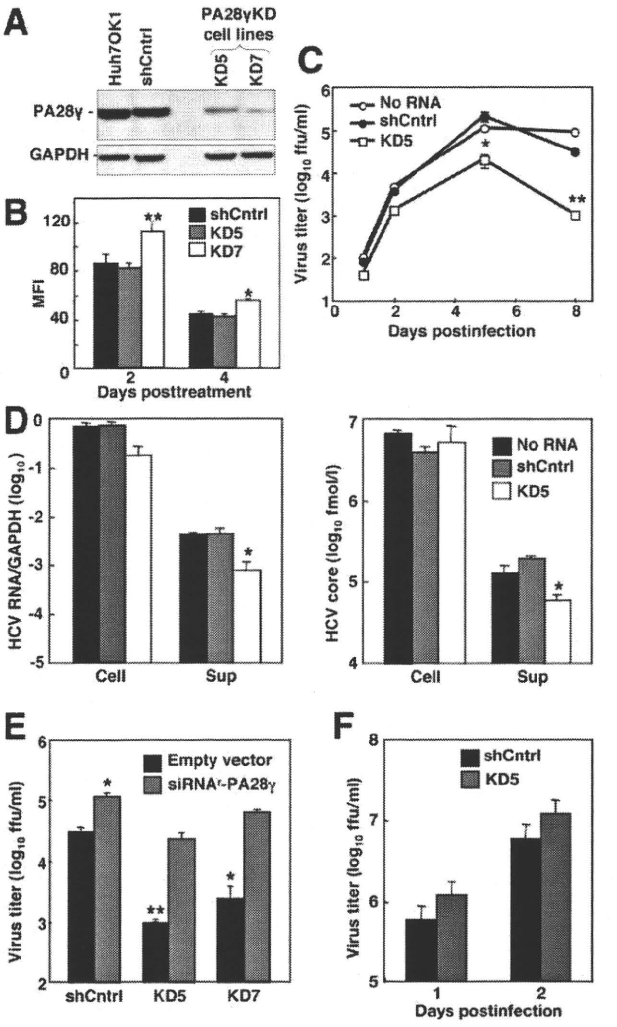

Fig. 2. Establishment of PA28γ knockdown cell lines and propagation of HCV. (A) Huh7OK1 cells were transfected with pSilencer shPA28γ or control plasmid and selected by hygromycin at 48 hours posttransfection. Two PA28γ knockdown cell lines (KD5 and KD7) and one control cell line (shCntrl) were established, and PA28γ knockdown was confirmed by way of immunoblotting. (B) Growth of the cell lines was determined by staining with carboxyfluorescein succinimidyl ester. (C,D) KD5 and shCntrl cell lines were infected with the JFH-1virus at an moi of 0.05. The infectious virus titers in the culture supernatants (C) was determined by way of focus-forming assay. The virus RNA (D, left panel) and the core protein (D, right panel) in both cell and the supernatant were determined at 5 days postinfection by way of ELISA and quantitative reverse-transcription polymerase chain reaction, respectively. (E) The plasmid encoding an siRNA-resistant PA28γ or empty vector was transfected into the cell lines, seeded at 5×10^4 cells into a six-well plate after cultivation in the presence of puromycin for 2 days, and infected with JFH-1 virus at an moi of 0.05. The viral titers were determined at 5 days postinfection. $^*P < 0.05$, $^{**}P < 0.01$ versus shCntrl cells transfected with an empty vector. (F). KD5 and shCntrl cell lines were infected with the JEV virus at an moi of 0.5. The infectivity of JEV in the supernatant was determined at 1 and 2 days postinfection. Data are representative of three independent experiments.

derived from the Con1 or JFH-1 strain induced no significant reduction of HCV RNA (Fig. 3A). Furthermore, luciferase activities in the stable PA28γ

knockdown cell line KD5 and the control cell line transfected with the subgenomic replicon RNA (WT) were gradually increased until 4 days posttransfection, whereas luciferase activities in the same two cell lines transfected with the polymerase-dead replicon RNA (GND) were decreased in a time-dependent manner (Fig. 3B). Next, to explore the effect of PA28γ knockdown on the viral replication over a longer period, replicon RNA encoding the neomycin-resistance gene was transfected into the cell lines for a colony formation assay. The numbers of colonies in the KD5 cell line after 4 weeks of selection with G418 were similar to those in the control cell line (Fig. 3C). To further clarify the roles of PA28γ on the postreplication steps, *in vitro* transcribed full-length viral RNA was transfected into Huh7OK1 cells, and siPA28γ1 was then introduced into the cells at 24 hours posttransfection of viral RNA. Intracellular core protein was increased in a time-dependent manner, but no significant difference was observed between cells transfected with control siRNA and those transfected with siPA28γ1 (Fig. 3D, left panel). However, infectious virus titers in the supernatant were significantly decreased by the transient and stable knockdown of PA28γ compared with control cells (Fig. 3D, middle and right panels). Furthermore, PA28γ did not contribute to the virus production of JEV (Fig. 2F), suggesting that the general sorting pathway of the flavivirus is functional under

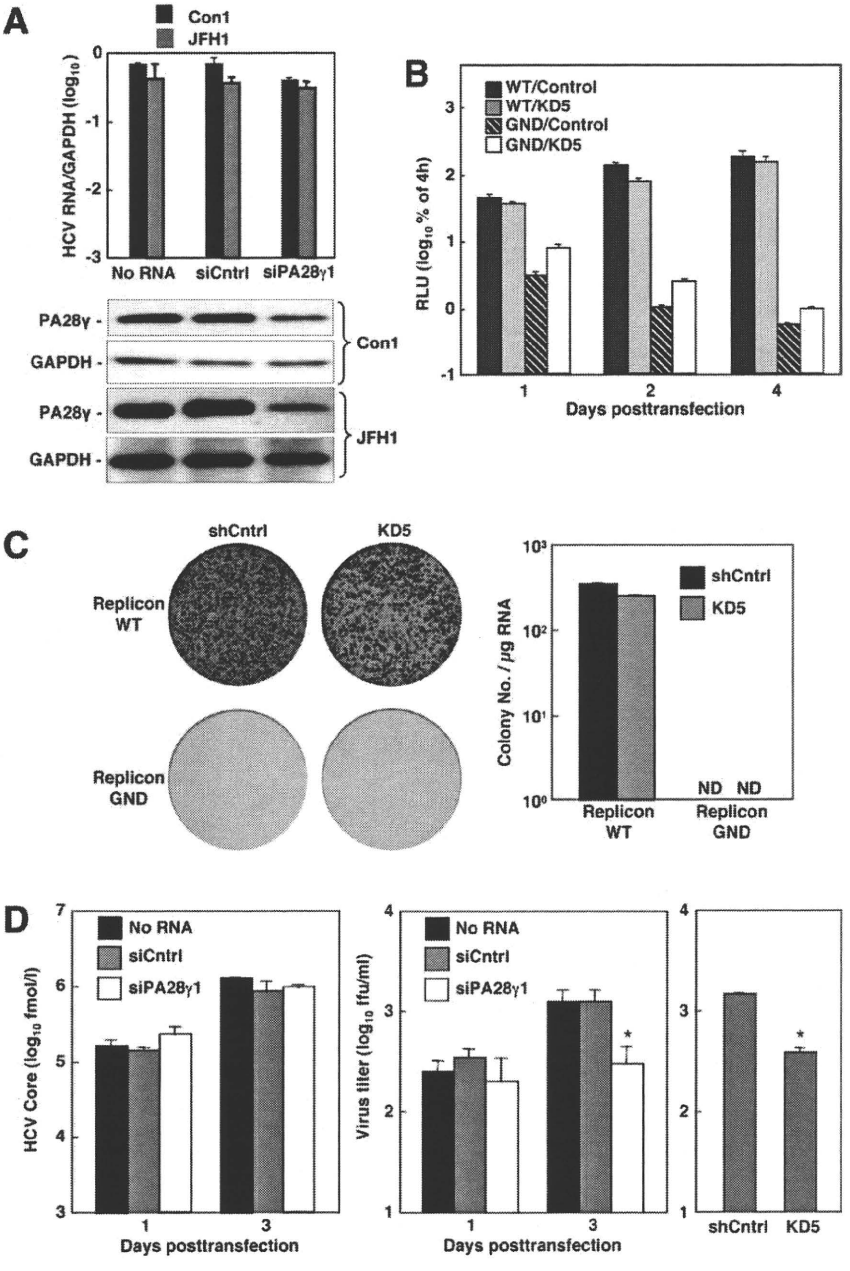

Fig. 3. Effect of PA28γ knockdown on HCV RNA replication. (A) The siCntrl or siPA28γ1 (10 nM) was transfected into the subgenomic HCV replicon cells derived from Con1 and JFH-1 strains. The transfected cells were harvested at 72 hours posttransfection. The replicon RNA was determined by quantitative reverse-transcription polymerase chain reaction at 72 hours posttransfection (upper). PA28γ or glyceraldehyde 3-phosphate dehydrogenase was detected by way of immunoblotting. Cell lysates were subjected to western blotting using antibodies to PA28γ and glyceraldehyde 3-phosphate dehydrogenase (lower). (B) The HCV replicon RNA encoding luciferase gene (WT) or the HCV replicon RNA that has a replication-deficient mutation (GND) was transfected into the shCntrl (Control) and KD5 cell lines. Relative luciferase activity was determined using the activity at 4 hours post-electroporation as a transfection efficiency. (C) Colony formation assay. Replicon RNA encoding the neomycin-resistance gene was transfected into the shCntrl and KD5 cell lines, and the remaining colonies were fixed with 4% paraformaldehyde at 4 weeks posttransfection and then stained with crystal violet. The number of colonies was counted (right). (D) Huh7OK1 cells transfected with 10 μg of *in vitro*-transcribed full-length JFH-1 viral RNA were further transfected with siCntrl or siPA28γ1 at 24 hours posttransfection of viral RNA. The level of HCV core protein in the cells was determined by way of ELISA at 1 and 3 days posttransfection (left). Infectious virus titers in the culture supernatants at 1 and 3 days posttransfection were determined by way of focus-forming assay (middle). Infectious viral titers in the shCntrl or KD5 cells transfected with 10 μg of the infectious viral RNA were determined at 5 days posttransfection (right). $^*P < 0.05$, $^{**}P < 0.01$ versus the control cells or cells transfected with siCntrl. Data are representative of three independent experiments.

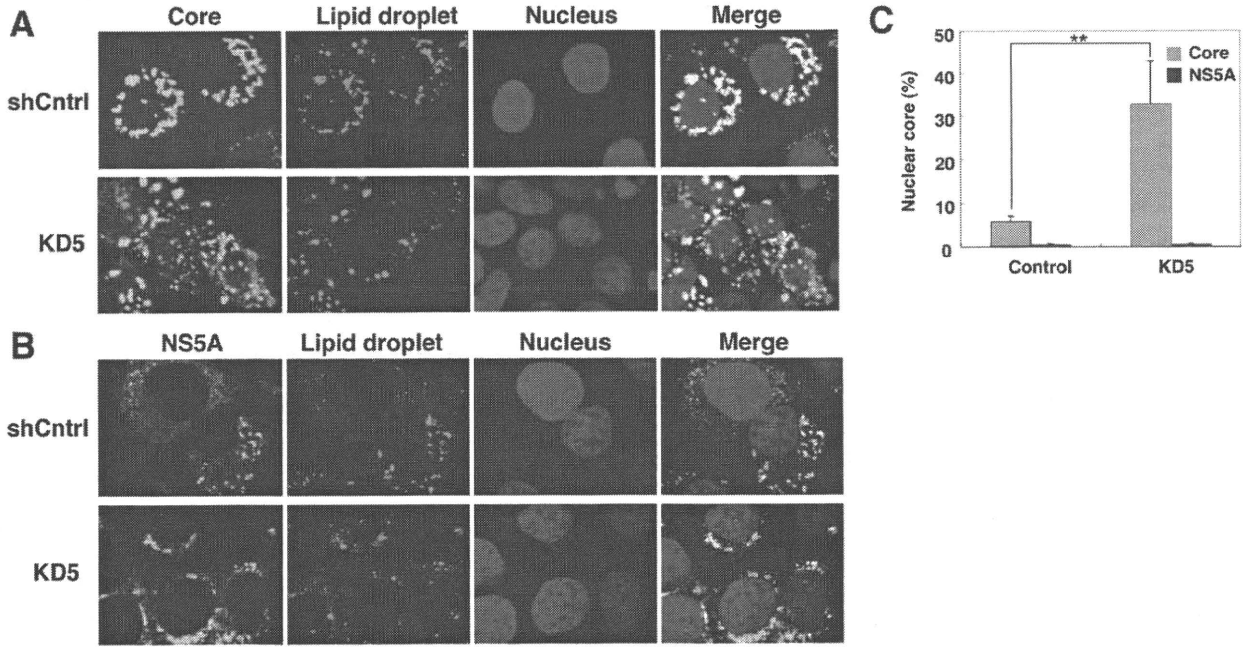

Fig. 4. Effect of PA28γ knockdown on the localization of HCV core protein and lipid droplets. The shCntrl and KD5 cell lines infected with JFH-1 virus were fixed with methanol or paraformaldehyde for 5 minutes at 4 days postinfection. HCV core (A) and NS5A (B) proteins were stained with rabbit antibodies raised against the proteins and Alexa Flour 488-conjugated goat anti-rabbit immunoglobulin G antibody. Lipid droplets were stained with Bodipy 558/568 C12. Nuclei were stained with 50 μM Heachest 33258 after treatment with 1 μg/mL of RNase A. Data are representative of three independent experiments. (C) The percentage of the area occupied by the core protein in nucleus and cytoplasm was calculated using the method described in Materials and Methods. The percentage of the nuclear NS5A to total NS5A was estimated by the same way as the ratio of the core protein. $^{**}P < 0.01$ versus control siRNA-transfected cells.

the PA28γ knockdown condition. These results suggest that PA28γ specifically regulates the postreplication steps in the life cycle of HCV.

Core Protein Is Partially Accumulated in the Nucleus of PA28γ Knockdown Cells. We reported previously that some fraction of HCV core protein migrates into the nucleus and is then degraded by a PA28γ-dependent proteasome pathway.[7] Furthermore, we have demonstrated that HCV core protein is clearly accumulated in the nucleus of the liver cells of PA28γ-knockout mice.[8] However, the role of PA28γ on the intracellular localization of HCV core protein in the infected HCV cells has not been characterized. HCV core protein was chiefly detected in cytoplasm of the control cell line infected with the JFH-1 virus, where it appeared around lipid droplets after staining with Bodipy 558/568 C12 (Fig. 4A, upper panels). In contrast, the core protein was detected not only in the cytoplasm around the surface of lipid droplets, but also in the nucleus in the KD5 cell line (Fig. 4A, lower panels). The NS5A protein was detected in the cytoplasm but not in the nucleus in both the shCntrl and KD5 cell lines (Fig. 4B). The percentage occupied by nuclear core protein to total core protein was increased by about six time levels in the KD5, while the ratio of nuclear NS5A to total NS5A exhibited no difference (Fig. 4C). These results suggest that PA28γ participates in the degradation of HCV core protein in the nucleus.

PA28γ Positively Regulates HCV Propagation by Inhibiting Ubiquitin-Dependent Degradation of Core Protein in Cytoplasm. We reported previously that HCV core protein is degraded by at least two distinct pathways: a ubiquitin-dependent proteasome pathway and a ubiquitin-independent proteasome pathway.[17] The ubiquitin E3 ligase, E6AP, can catalyze ubiquitin ligation of the core protein for ubiquitin-dependent degradation in the cytoplasm,[18] whereas PA28γ participates in the degradation of the core protein through a ubiquitin-independent pathway in the nucleus.[17] We have also demonstrated that PA28γ knockdown leads to enhanced ubiquitination of HCV core protein.[8] However, the interplay between these two pathways in cells infected with HCV has not been determined. To address this point, we examined the effects of knockdown of E6AP or PA28γ on the virus propagation and the ubiquitination of the core protein. JFH-1 virus was inoculated into E6AP- and/or PA28γ knockdown cell lines (Fig. 5A). Transfection of the plasmid encoding shRNA to E6AP into the control cells (shCntrl) increased virus production (Fig. 5A [C-E]) in comparison with that of the

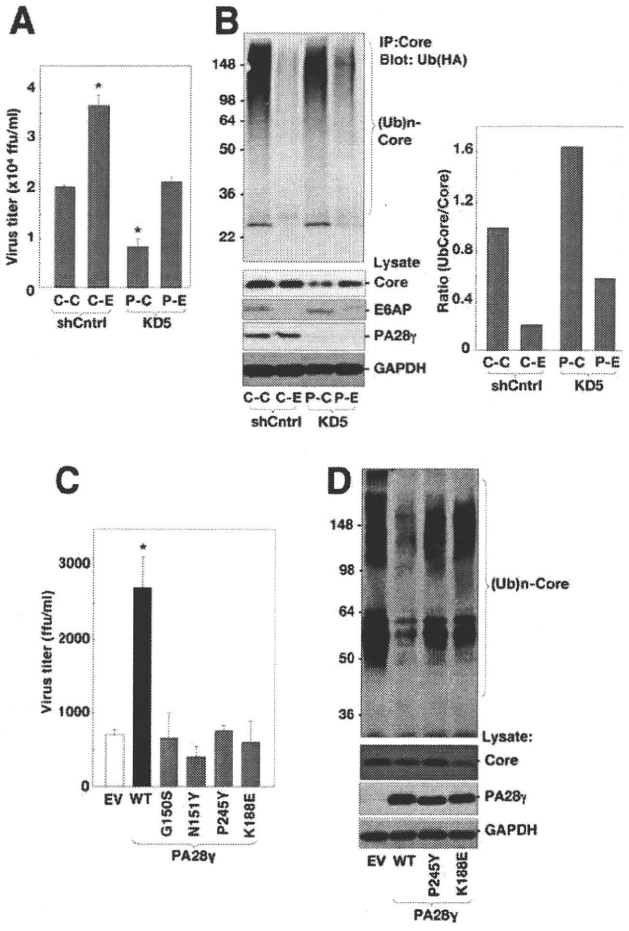

Fig. 5. PA28γ knockdown enhances E6AP-dependent ubiquitination of core protein and reduces virus titer. (A) shCntrl and KD5 cells transfected with plasmids encoding the negative control (C-C and P-C) or E6AP (C-E and P-E) shRNA were treated with puromycin for 2 days. The remaining cells seeded at 2.5×10^4 cells in a 24-well plate were infected with the JFH-1 virus at an moi of 0.05, and infectious virus titers in the supernatants were determined at 72 hours postinfection by way of focus-forming assay. (B) The cells transfected and infected as in (A) were further transfected with a plasmid encoding HA-tagged ubiquitin at 48 hours postinfection. The cells were treated with 10 μM MG132 for 5 hours at 72 hours postinfection and subjected to immunoprecipitation with anti-core monoclonal antibody and immunoblotting with anti-HA antibody. The ratio of ubiquitination of HCV core protein was assessed by the densitometries of the ubiquitinated and unubiquitinated core proteins. (C) KD5 cells transfected with plasmids encoding wild-type or mutant PA28γ were infected with the JFH-1 virus at an moi of 0.05 at 24 hours posttransfection, and the infectious titers in the supernatant were determined at 72 hours postinfection by way of focus-forming assay. (D) KD5 cells transfected with plasmids encoding HCV core protein and HA-tagged ubiquitin, together with wild-type or mutant PA28γ, were treated with 10 μM MG132 for 5 hours at 24 hours posttransfection and subjected to immunoprecipitation with anti-core monoclonal antibody and immunoblotting with anti-HA antibody. EV, empty vector; WT, plasmid encoding wild-type PA28γ. $^*P < 0.05$ versus shCntrl or KD5 cells transfected with the negative control or empty vector. Data are representative of three independent experiments.

control cells transfected with the plasmid encoding control shRNA (Fig. 5A [C-C]). Furthermore, the impaired virus production in the PA28γ knockdown cells (KD5) was restored by the transfection of the plasmid encoding shRNA to E6AP (Fig. 5A [P-E]). Cells expressing hemagglutinin (HA)-tagged ubiquitin infected with the JFH-1 virus were immunoprecipitated by the anti-core antibody, and the immunoprecipitates were analyzed by immunoblotting with anti-HA antibody (Fig. 5B). E6AP knockdown decreased the ratio of ubiquitination of HCV core protein, in contrast to the increase of that by PA28γ knockdown (Fig. 5B, lanes C-E and P-C). Furthermore, E6AP knockdown in the PA28γ knockdown cells restored the ubiquitination of the core protein to a certain extent (Fig. 5B, lane P-E). It was shown that Pro^{245} of PA28γ is critical for binding to the 20S proteasome, and that Gly^{150} and Asn^{151} of PA28γ are important for activation of the proteasome.[26] To further examine the functional significance of PA28γ on HCV propagation, expression plasmids encoding siRNA-resistant PA28γ mutants in which Gly^{150}, Asn^{151}, and Pro^{245} were replaced with Ser (G150S), Tyr (N151Y), and Tyr (P245Y), respectively, were transfected into KD5 cells and inoculated with JFH-1 virus at 24 hours posttransfection. The infectious virus titers in the culture supernatant were determined at 3 days postinfection (Fig. 5C). KD5 cells transfected with the plasmid encoding wild-type PA28γ exhibited a partial recovery of virus production, although those transfected with the plasmid encoding PA28γ G150S, N151Y, or P245Y or with an empty vector exhibited no effect on virus production. Replacing Lys^{188} with Glu in PA28γ (PA28γ K188E) confers the capability of proteasome-mediated cleavage after hydrophobic, acidic, and basic residues such as those exhibited by PA28α.[27] Expression of siRNA-resistant PA28γ K188E in KD5 cells could not restore virus production (Fig. 5D). The ubiquitination of HCV core protein was inhibited by expression of the wild-type PA28γ but not expression of the PA28γ mutants (P245Y or K188E) in KD5 cells (Fig. 5D). Collectively, these results suggest that PA28γ positively regulates HCV propagation by inhibiting degradation of HCV core protein by an E6AP/ubiquitin-dependent proteasome.

Discussion

To explore the role of PA28γ on the life cycle of HCV, we examined the effects of knockdown of PA28γ in Huh7OK1 cells infected with the JFH-1 virus. Knockdown of PA28γ in Huh7OK1 cells before or after infection with the JFH-1 virus impaired

production of infectious particles but did not impair viral RNA replication. However, PA28γ knockdown did not affect the production of JEV, of which the capsid protein does not interact with PA28γ, suggesting that PA28γ knockdown does not affect the general sorting pathway of flavivirus. These results suggest that PA28γ is specifically involved in the postreplication steps of HCV life cycle. Our previous report indicated that HCV core protein was accumulated in the nucleus of the hepatocytes of HCV core transgenic/PA28γ knockout mice.[8] PA28γ is located mainly in the nucleus, although a small portion is also located in the cytoplasm[7,28] and can up-regulate trypsin-like proteasome activity, which cleaves after basic amino acid residues.[27] Previous studies have shown that some fraction of HCV core protein is translocated into the nucleus and quickly degraded in the PA28γ-dependent proteasome pathway.[7,8,29] Miyanari et al.[30] demonstrated that the core protein is localized on the surface of lipid droplets and is surrounded by nonstructural proteins, suggesting that HCV particles are assembled near the surface of the lipid droplets. In the present experiments, although HCV core protein was detected on the surface of the lipid droplets in both control and PA28γ knockdown cell lines, it was partially localized in the nucleus in PA28γ knockdown cells but not control cells. Furthermore, localization of HCV core protein on the surface of lipid droplets was impaired in PA28γ knockdown cells (Fig. 4). These results suggest that HCV core protein is partially translocated into the nucleus and degraded in the PA28γ-dependent proteasome pathway in HCV-infected cells and that PA28γ does not directly participate in the particle formation of HCV.

HCV core protein is degraded by at least two proteasome pathways: a ubiquitin-dependent pathway and a ubiquitin-independent and PA28γ-dependent pathway.[17] The E3 ligase E6AP catalyzes ubiquitin ligation to HCV core protein, resulting in enhanced degradation of the core protein in the cytoplasm.[18] Knockdown of E6AP up-regulated virus production in cells infected with the JFH-1 virus,[18] suggesting that E6AP/ubiquitin-dependent degradation of the core protein contributes to an antiviral response. In contrast, knockdown of PA28γ induced up-regulation of the ubiquitination of HCV core protein and down-regulation of the viral production, suggesting that PA28γ-dependent proteasome activity contributes to the proviral response by suppressing E6AP-dependent degradation of the core protein, thereby enhancing viral particle formation. The wild-type PA28γ enhances the trypsin-like activity of proteasome that cleaves peptide bonds after basic residues of the substrates, whereas the PA28γ K188E mutant enhances the proteasome activity that cleaves peptide bonds after hydrophobic, acidic, and basic residues in the manner of PA28α.[27] Therefore, the sizes of fragments produced by the PA28γ-dependent proteasome should be different from those produced by the PA28α/β- or ubiquitination-mediated proteasome. It might be feasible to speculate that the peptide fragments of HCV core protein generated by the PA28γ-dependent proteasome or PA28γ *per se* may be directly or indirectly involved in the suppression of the E6AP-dependent ubiquitination of the core protein. Further studies will be needed to clarify the relationship between E6AP and PA28γ in the degradation and ubiquitination of HCV core protein. Figure 6 shows a schematic diagram of our hypothesis of the regulation of HCV propagation by PA28γ.

HCV core protein was found in not only nuclei but also cytoplasm of the infected KD5 cells (Fig. 4). The down-regulation of virus production should potently reduce a total amount of the core protein in KD5 cells before a clear accumulation of the core protein in nuclei. Furthermore, a small amount of PA28γ was found in the PA28γ knockdown cells, suggesting that E6AP-dependent degradation of HCV core protein is not potently suppressed in the PA28γ knockdown cells. If HCV core protein is constitutively expressed under the PA28γ knockout cells regardless of an amount of infected virus, a clear accumulation of the core protein in nuclei should be found without cytoplasmic expression of the core protein under the PA28γ knockout condition. We reported previously that HCC and liver steatosis in mouse are induced by the HCV core protein in the presence, but not the absence, of PA28γ.[8] Although HCV core protein is predominantly detected in the cytoplasm of the liver cells of PA28$\gamma^{+/+}$ mice,[8,31] HCV core protein was clearly accumulated in the nuclei, but clearly reduced in cytoplasm, of liver cells of PA28$\gamma^{-/-}$ mouse.[8] In addition, ubiquitination of HCV core protein was increased by PA28γ knockdown in the 293T cell line.[8] These results and the data in Fig. 5 suggest that the suppression of PA28γ function enhances the E6AP-dependent degradation of HCV core protein. Hence, the reason there is no difference between PA28$\gamma^{+/+}$ and PA28$\gamma^{-/-}$ mice with respect to the amount of core protein may be due to the competitive regulation of the core protein by E6AP- and PA28γ-dependent degradation mechanisms. E6AP-dependent degradation of HCV core protein in cytoplasm may be enhanced *in vivo* under the PA28γ knockout condition.

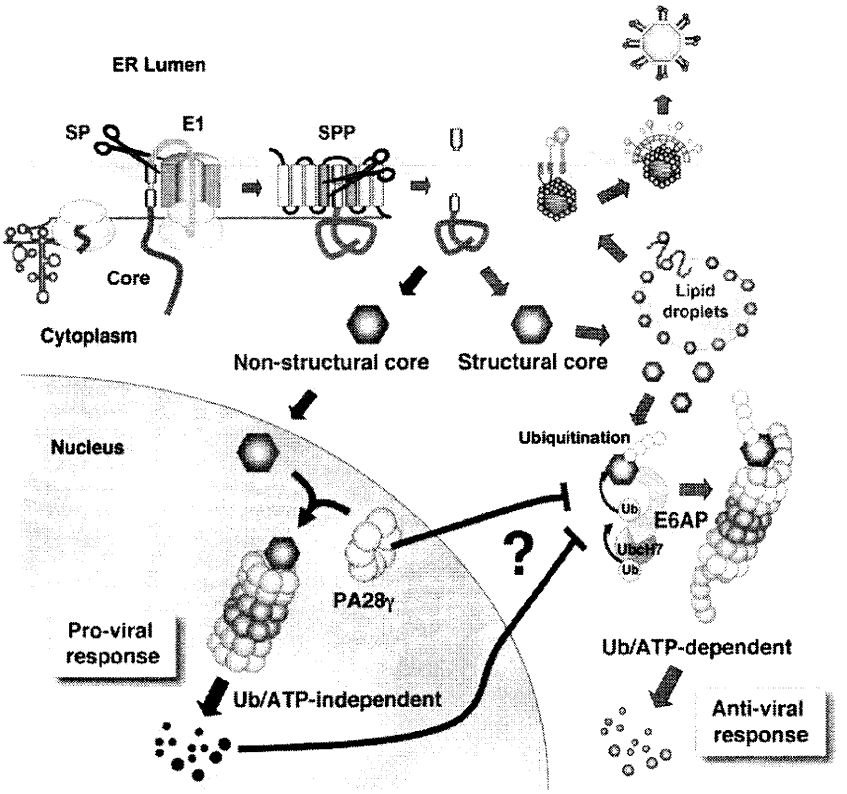

Fig. 6. Schematic diagram of the potential roles of PA28γ in HCV propagation. HCV core protein is cleaved off from the precursor polyprotein by signal peptidase (SP) and the signal sequence is further processed by signal peptide peptidase (SPP). The mature core protein mainly localizes on the lipid droplets close to the endoplasmic reticulum to form a nucleocapsid with the viral RNA genome and is incorporated into virus particles as a structural protein. In addition to the structural protein of HCV, the core protein has characteristics of a nonstructural protein. HCV core protein is degraded through ubiquitin-dependent and ubiquitin-independent proteasome pathways. E6AP catalyzes ubiquitin ligation to HCV core protein and promotes degradation in the cytoplasm, which contributes to the antiviral response. In contrast, the core protein partially migrates into the nucleus and is degraded through a ubiquitin-independent and PA28γ-dependent proteasome pathway, and the core protein fragments generated by the PA28γ pathway or PA28γ *per se* were suggested to participate in the suppression of E6AP-dependent ubiquitination of HCV core protein, which contributes to the proviral response.

In conclusion, in this study we demonstrated that the proteasome activator PA28γ positively regulates particle production of HCV by inhibiting E6AP-dependent ubiquitination of the core protein, in addition to our previous observation that PA28γ plays a crucial role in the development of liver pathology induced by HCV core protein.[8] PA28γ knockout mice exhibit only mild growth retardation.[15,16] Therefore, PA28γ may be a novel and promising antiviral target not only for elimination of HCV from hepatitis C patients but also for intervention in the progression of liver diseases induced by chronic HCV infection.

Acknowledgment: We thank H. Murase for her secretarial work. We also thank R. Bartenschlager and T. Wakita for providing cell lines and plasmids.

References

1. Wasley A, Alter MJ. Epidemiology of hepatitis C: geographic differences and temporal trends. Semin Liver Dis 2000;20:1-16.
2. Moriishi K, Matsuura Y. Host factors involved in the replication of hepatitis C virus. Rev Med Virol 2007;17:343-354.
3. Hussy P, Langen H, Mous J, Jacobsen H. Hepatitis C virus core protein: carboxy-terminal boundaries of two processed species suggest cleavage by a signal peptide peptidase. Virology 1996;224:93-104.
4. Okamoto K, Mori Y, Komoda Y, Okamoto T, Okochi M, Takeda M, et al. Intramembrane processing by signal peptide peptidase regulates the membrane localization of hepatitis C virus core protein and viral propagation. J Virol 2008;82:8349-8361.
5. Barba G, Harper F, Harada T, Kohara M, Goulinet S, Matsuura Y, et al. Hepatitis C virus core protein shows a cytoplasmic localization and associates to cellular lipid storage droplets. Proc Natl Acad Sci U S A 1997;94:1200-1205.
6. Moriya K, Yotsuyanagi H, Shintani Y, Fujie H, Ishibashi K, Matsuura Y, et al. Hepatitis C virus core protein induces hepatic steatosis in transgenic mice. J Gen Virol 1997;78:1527-1531.
7. Moriishi K, Okabayashi T, Nakai K, Moriya K, Koike K, Murata S, et al. Proteasome activator PA28gamma-dependent nuclear retention and degradation of hepatitis C virus core protein. J Virol 2003;77:10237-10249.
8. Moriishi K, Mochizuki R, Moriya K, Miyamoto H, Mori Y, Abe T, et al. Critical role of PA28gamma in hepatitis C virus-associated steatogenesis and hepatocarcinogenesis. Proc Natl Acad Sci U S A 2007;104:1661-1666.
9. Miyamoto H, Moriishi K, Moriya K, Murata S, Tanaka K, Suzuki T, et al. Involvement of PA28gamma-dependent pathway in insulin resistance induced by hepatitis C virus core protein. J Virol 2007;81:1727-1735.

10. Li X, Lonard D, Jung SY, Malovannaya A, Feng Q, Qin J, et al. The SRC-3/AIB1 coactivator is degraded in a ubiquitin- and ATP-independent manner by the REGgamma proteasome. Cell 2006;124: 381-392.
11. Zhang Z, Zhang R. Proteasome activator PA28 gamma regulates p53 by enhancing its MDM2-mediated degradation. EMBO J 2008;27: 852-864.
12. Chen X, Barton LF, Chi Y, Clurman BE, Roberts JM. Ubiquitin-independent degradation of cell-cycle inhibitors by the REGgamma proteasome. Mol Cell 2007;26:843-852.
13. Li X, Amazit L, Long W, Lonard DM, Monaco JJ, O'Malley BW. Ubiquitin- and ATP-independent proteolytic turnover of p21 by the REGgamma-proteasome pathway. Mol Cell 2007;26:831-842.
14. Jariel-Encontre I, Bossis G, Piechaczyk M. Ubiquitin-independent degradation of proteins by the proteasome. Biochim Biophys Acta 2008; 1786:153-177.
15. Barton LF, Runnels HA, Schell TD, Cho Y, Gibbons R, Tevethia SS, et al. Immune defects in 28-kDa proteasome activator gamma-deficient mice. J Immunol 2004;172:3948-3954.
16. Murata S, Kawahara H, Tohma S, Yamamoto K, Kasahara M, Nabeshima Y, et al. Growth retardation in mice lacking the proteasome activator PA28gamma. J Biol Chem 1999;274:38211-38215.
17. Suzuki R, Moriishi K, Fukuda K, Shirakura M, Ishii K, Shoji I, et al. Proteasomal turnover of hepatitis C virus core protein is regulated by two distinct mechanisms: a ubiquitin-dependent mechanism and a ubiquitin-independent but PA28gamma-dependent mechanism. J Virol 2009;83:2389-2392.
18. Shirakura M, Murakami K, Ichimura T, Suzuki R, Shimoji T, Fukuda K, et al. E6AP ubiquitin ligase mediates ubiquitylation and degradation of hepatitis C virus core protein. J Virol 2007;81:1174-1185.
19. Aoyagi K, Ohue C, Iida K, Kimura T, Tanaka E, Kiyosawa K, et al. Development of a simple and highly sensitive enzyme immunoassay for hepatitis C virus core antigen. J Clin Microbiol 1999;37:1802-1808.
20. Lohmann V, Korner F, Koch J, Herian U, Theilmann L, Bartenschlager R. Replication of subgenomic hepatitis C virus RNAs in a hepatoma cell line. Science 1999;285:110-113.
21. Wakita T, Pietschmann T, Kato T, Date T, Miyamoto M, Zhao Z, et al. Production of infectious hepatitis C virus in tissue culture from a cloned viral genome. Nat Med 2005;11:791-796.
22. Pietschmann T, Lohmann V, Kaul A, Krieger N, Rinck G, Rutter G, et al. Persistent and transient replication of full-length hepatitis C virus genomes in cell culture. J Virol 2002;76:4008-4021.
23. Mori Y, Okabayashi T, Yamashita T, Zhao Z, Wakita T, Yasui K, et al. Nuclear localization of Japanese encephalitis virus core protein enhances viral replication. J Virol 2005;79:3448-3458.
24. Targett-Adams P, Chambers D, Gledhill S, Hope RG, Coy JF, Girod A, et al. Live cell analysis and targeting of the lipid droplet-binding adipocyte differentiation-related protein. J Biol Chem 2003;278: 15998-16007.
25. Okamoto T, Omori H, Kaname Y, Abe T, Nishimura Y, Suzuki T, et al. A single-amino-acid mutation in hepatitis C virus NS5A disrupting FKBP8 interaction impairs viral replication. J Virol 2008;82: 3480-3489.
26. Zhang Z, Clawson A, Realini C, Jensen CC, Knowlton JR, Hill CP, et al. Identification of an activation region in the proteasome activator REGalpha. Proc Natl Acad Sci U S A 1998;95:2807-2811.
27. Li J, Gao X, Ortega J, Nazif T, Joss L, Bogyo M, et al. Lysine 188 substitutions convert the pattern of proteasome activation by REGgamma to that of REGs alpha and beta. EMBO J 2001;20:3359-3369.
28. Nikaido T, Shimada K, Nishida Y, Lee RS, Pardee AB, Nishizuka Y. Loss in transformed cells of cell cycle regulation of expression of a nuclear protein recognized by SLE patient antisera. Exp Cell Res 1989; 182:284-289.
29. Suzuki R, Sakamoto S, Tsutsumi T, Rikimaru A, Tanaka K, Shimoike T, et al. Molecular determinants for subcellular localization of hepatitis C virus core protein. J Virol 2005;79:1271-1281.
30. Miyanari Y, Atsuzawa K, Usuda N, Watashi K, Hishiki T, Zayas M, et al. The lipid droplet is an important organelle for hepatitis C virus production. Nat Cell Biol 2007;9:1089-1097.
31. Moriya K, Fujie H, Shintani Y, Yotsuyanagi H, Tsutsumi T, Ishibashi K, et al. The core protein of hepatitis C virus induces hepatocellular carcinoma in transgenic mice. Nat Med 1998;4:1065-1067.

ARTICLE

Journal of Cellular Biochemistry 111:676–685 (2010)

Journal of Cellular Biochemistry

E6AP Ubiquitin Ligase Mediates Ubiquitin-Dependent Degradation of Peroxiredoxin 1

Junichi Nasu,[1,2] Kyoko Murakami,[1] Shoji Miyagawa,[3] Ryosuke Yamashita,[3] Tohru Ichimura,[4] Takaji Wakita,[1] Hak Hotta,[3] Tatsuo Miyamura,[1] Tetsuro Suzuki,[1] Tazuko Satoh,[2] and Ikuo Shoji[1,3*]

[1] *Department of Virology II, National Institute of Infectious Diseases, Shinjuku-ku, Tokyo, Japan*

[2] *Department of Oral and Maxillofacial Surgery, School of Life Dentistry at Tokyo, the Nippon Dental University, Chiyoda-ku, Tokyo, Japan*

[3] *Division of Microbiology, Center for Infectious Diseases, Kobe University Graduate School of Medicine, Kobe, Hyogo, Japan*

[4] *Department of Applied Chemistry, National Defense Academy, Yokosuka, Kanagawa, Japan*

ABSTRACT

E6-associated protein (E6AP) is a cellular ubiquitin protein ligase that mediates ubiquitylation and degradation of tumor suppressor p53 in conjunction with the high-risk human papillomavirus E6 protein. We previously reported that E6AP targets annexin A1 protein for ubiquitin-dependent proteasomal degradation. To gain a better understanding of the physiological function of E6AP, we have been seeking to identify novel substrates of E6AP. Here, we identified peroxiredoxin 1 (Prx1) as a novel E6AP-binding protein using a tandem affinity purification procedure coupled with mass spectrometry. Prx1 is a 25-kDa member of the Prx family, a ubiquitous family of antioxidant peroxidases that regulate many cellular processes through intracellular oxidative signal transduction pathways. Immunoprecipitation analysis showed that E6AP binds Prx1 in vivo. Pull-down experiments showed that E6AP binds Prx1 in vitro. Ectopic expression of E6AP enhanced the degradation of Prx1 in vivo. In vivo and in vitro ubiquitylation assays revealed that E6AP promoted polyubiquitylation of Prx1. RNAi-mediated downregulation of endogenous E6AP increased the level of endogenous Prx1 protein. Taken together, our data suggest that E6AP mediates the ubiquitin-dependent proteasomal degradation of Prx1. Our findings raise a possibility that E6AP may play a role in regulating Prx1-dependent intracellular oxidative signal transduction pathways. J. Cell. Biochem. 111: 676–685, 2010.

KEY WORDS: E6AP; Prx1; UBIQUITIN; DEGRADATION

E6-associated protein (E6AP) is the prototype of a family of ubiquitin ligases called HECT domain ubiquitin ligases, all of which contain a domain homologous to the E6AP carboxyl terminus [Huibregtse et al., 1995]. E6AP was initially identified as the cellular factor that stimulates ubiquitin-dependent degradation of the tumor suppressor p53 in conjunction with the E6 protein of cervical cancer-associated human papillomavirus (HPV) types 16 and 18 [Huibregtse et al., 1993; Scheffner et al., 1994]. The E6–E6AP complex functions as an E3 ubiquitin ligase in the ubiquitylation of p53 [Scheffner et al., 1993]. Known substrates of the E6–E6AP complex include the tumor suppressor p53 [Scheffner et al., 1993], the PDZ domain-containing protein Scribble [Nakagawa and Huibregtse, 2000], and NFX1-91, a transcriptional repressor of the gene encoding hTERT [Gewin et al., 2004]. The ability of E6 to

Abbreviations: E6AP, E6-associated protein; Prx, peroxiredoxin; HPV, human papillomavirus; MS, mass spectrometry; MAb, monoclonal antibody; PAb, polyclonal antibody; GAPDH, glyceraldehydes-3-phosphate dehydrogenase; CHX, cycloheximide.

Grant sponsor: The Nippon Dental University; Grant sponsor: Japan Health Sciences Foundation; Grant sponsor: Ministry of Health, Labour, and Welfare; Grant sponsor: Ministry of Education, Science and Culture of Japan; Grant sponsor: Program for Promotion of Fundamental Studies in Health Sciences of the National Institute of Biomedical Innovation (NIBIO), Japan.

*Correspondence to: Dr. Ikuo Shoji, MD, PhD, Division of Microbiology, Center for Infectious Diseases, Kobe University Graduate School of Medicine, 7-5-1 Kusunoki-cho, Chuo-ku, Kobe, Hyogo 650-0017, Japan.
E-mail: ishoji@med.kobe-u.ac.jp

Received 7 March 2010; Accepted 15 June 2010 • DOI 10.1002/jcb.22752 • © 2010 Wiley-Liss, Inc.
Published online 29 June 2010 in Wiley Online Library (wileyonlinelibrary.com).

utilize E6AP to target p53 and other cellular proteins for degradation contributes to its oncogenic functions [Matentzoglu and Scheffner, 2008]. Interestingly, E6AP is not involved in the ubiquitylation of p53 in the absence of E6 [Talis et al., 1998].

In an attempt to understand the physiological function of E6AP, several potential E6-independent substrates for E6AP have been identified, such as HHR23A and HHR23B (the human orthologs of *Saccharomyces cerevisae* Rad23) [Kumar et al., 1999], Blk (a member of the Src family kinases) [Oda et al., 1999], Mcm7 (which is involved in DNA replication) [Kuhne and Banks, 1998], trihydrophobin 1 [Yang et al., 2007], and AIB1 (a steroid receptor coactivator) [Mani et al., 2006]. We previously reported that E6AP mediates ubiquitylation and degradation of annexin A1 in a Ca^{2+}-dependent manner [Shimoji et al., 2009].

Some patients with Angelman syndrome, a severe neurological disorder linked to E6AP, have mutations within the catalytic cleft that have been shown to reduce E6AP ubiquitin ligase activity [Kishino et al., 1997; Matsuura et al., 1997; Cooper et al., 2004]. Despite the significant progress in the study of Angelman syndrome-associated E6AP mutations, none of the identified E6AP substrates have been directly linked to the disorder. Much research is still needed to fully understand the functional links between lack of E6AP expression and clinical manifestations of Angelman syndrome [Dan, 2009]. We previously reported that E6AP mediates ubiquitin-dependent proteasomal degradation of hepatitis C virus (HCV) core protein, thereby affecting the production of HCV particles [Shirakura et al., 2007; Suzuki et al., 2009]. It is becoming increasingly clear that E6AP plays important roles in human diseases, such as cervical cancer, Angelman syndrome, and hepatitis C [Scheffner et al., 1993; Kishino et al., 1997; Shirakura et al., 2007].

In this study, we attempted to identify the novel functions of E6AP. We screened for potential binding partners for E6AP. A tandem affinity purification procedure coupled with mass spectrometry analysis identified peroxiredoxin 1 (Prx1) as a novel binding partner for E6AP. We provide evidence suggesting that E6AP mediates the ubiquitin-dependent proteasomal degradation of Prx1.

MATERIALS AND METHODS

CELL CULTURE AND TRANSFECTION

Human embryonic kidney (HEK) 293T cells were cultured in Dulbecco's modified Eagle's medium (DMEM; Sigma-Aldrich, St. Louis, MO) supplemented with 50 IU/ml penicillin, 50 μg/ml streptomycin (Invitrogen, Carlsbad, CA), and 10% (v/v) fetal bovine serum (FBS; JRH Biosciences, Lenexa, KS) at 37°C in a 5% CO_2 incubator. HEK293T cells were transfected with plasmid DNA using TransIT-LT1 (Mirus, Madison, WI).

PLASMIDS AND RECOMBINANT BACULOVIRUSES

To make a fusion protein consisting of hexahistidine (His_6)-tag fused to the N-terminus of Prx1 in *Escherichia coli*, pET17b-Prx1 [Kang et al., 1998] was digested with *Nde*I and *Bam*HI, and a Prx1 fragment was subcloned into the *Nde*I-Bpu1120I site of pET19b, resulting in pET19b-Prx1. The expression plasmid pET19b-Prx2 was constructed similarly. The plasmids, pET17b-Prx1 and pET17b-Prx2, were kind gifts from Dr. S.G. Rhee, Ewha Women's University, Korea.

To express the Prx1 protein as a FLAG-tagged fusion protein in mammalian cells, pCAG-FLAG-Prx1 was constructed as follows. The DNA fragment of Prx1 was amplified from pET17b-PrxI by polymerase chain reaction (PCR) using two oligonucleotides, 5′-GCGGCCGCCCACCATGGACTACAAAGACGATGACGATAAAGG-AGGCGGCGGATCCATGTCTTCAGGAAATGC-3′ and 5′-AGATCTT-CACTTCTGCTTGGAG-3′. To express FLAG-tagged Prx2 protein in mammalian cells, the DNA fragment of Prx2 was amplified from pET17b-Prx2 by PCR using two oligonucleotides, 5′-GCGGCCG-CCCACCATGGACTACAAAGACGATGACGATAAAGGAGGCGGCG-GATCCATGGCCTCCGGTAACGC-3′ and 5′-AGATCTCTAATTGTG-TTTGGAG-3′. The amplified PCR fragments were subcloned into pGEM T-Easy (Promega, Madison, WI) and verified by sequencing. Then the Prx1 and Prx2 gene fragments were digested with *Not*I and *Bgl*II, and ligated into the *Not*I–*Bgl*II site of pCAG-MCS2 [Shirakura et al., 2007]. The MEF-tag cassette (containing Myc-tag, the tobacco etch virus protease cleavage site, and FLAG-tag) was fused to the N-terminus of the cDNA encoding E6AP [Ichimura et al., 2005; Shirakura et al., 2007]. MEF-tagged E6AP and MEF-tagged E6AP C-A were subcloned into pcDNA3, pCAGGS, and pVL1392. pCAG-HA-E6AP, pCAG-HA-E6AP C-A, and pCAG-HA-Nedd4 were described previously [Shirakura et al., 2007; Shimoji et al., 2009]. The ubiquitin expression plasmids, pRK5-HA-Ubiquitin wild type (WT), pRK5-HA-Ubiquitin-K48R, and pRK5-HA-Ubiquitin-K48 [Lim et al., 2005], were provided by Dr. T. Dawson (Johns Hopkins University, MD).

ANTIBODIES

The mouse monoclonal antibodies (MAbs) used in this study were anti-hemagglutinin (HA) MAb (12CA5; Roche, Mannheim, Germany), anti-HA MAb (16B12; Covance, Princeton, NJ), anti-FLAG M2 mouse MAb (Sigma-Aldrich), anti-glyceraldehyde-3-phosphate dehydrogenase (GAPDH) MAb (Chemicon, Temecula, CA), anti-E6AP MAb (E6AP-330; Sigma-Aldrich), and anti-polyhistidine (His-1) MAb (Sigma-Aldrich). The c-Myc tagged protein mild purification kit (MBL) was used for immunoprecipitation. The polyclonal antibodies (PAbs) used in this study were anti-HA rabbit PAb (Y-11; Santa Cruz Biotechnology, Santa Cruz, CA), anti-FLAG rabbit PAb (F7425; Sigma-Aldrich), anti-Prx1 rabbit PAb (ab16805-100) (Abcam, Cambridge, Oxford), and anti-GST goat PAb (Amersham, Buckinghamshire, UK).

EXPRESSION AND PURIFICATION OF RECOMBINANT PROTEINS

E. coli BL21 (DE3) cells were transformed with plasmids expressing His_6-tagged protein and grown at 37°C. Expression of the fusion protein was induced by 1 mM isopropyl-β-D-thiogalactopyranoside (IPTG) at 25°C for 4 h. Bacteria were harvested, suspended in lysis buffer [50 mM Na_2HPO_4, 300 mM NaCl, 5 mM Imidazole, 0.1% Triton X-100, protease inhibitor cocktail (Complete EDTA-free; Roche)], and sonicated on ice. His_6-tagged proteins were purified on Ni-NTA beads (Qiagen, Hilden, Germany) according to the manufacturer's protocols. The MEF-E6AP and MEF-E6AP C-A were purified on anti-FLAG M2 agarose beads (Sigma-Aldrich) as described previously [Shirakura et al., 2007].

PURIFICATION OF E6AP-BINDING PROTEINS BY MEF PURIFICATION PROCEDURE

HEK293T cells were transfected with the plasmid expressing MEF-E6AP C-A by the calcium phosphate precipitation method, and the E6AP-binding proteins were recovered following the procedure described previously [Ichimura et al., 2005]. The inactive form of E6AP was expressed to inhibit ubiquitin-dependent degradation of potential substrates. Bound proteins were separated by 7.5% sodium dodecyl sulfate-polyacrylamide gel electrophoresis (SDS-PAGE) and visualized by silver staining. The stained bands were excised and digested in the gel with lysylendoprotease-C (Lys-C), and the resulting peptide mixtures were analyzed using a direct nanoflow liquid chromatography-tandem mass spectrometry (MS/MS) system, equipped with an electrospray interface reversed-phase column, a nanoflow gradient device, a high-resolution Q-time of flight hybrid mass spectrometer (Q-TOF2; Micromass, Manchester, UK), and an automated data analysis system [Natsume et al., 2002; Shirakura et al., 2007]. All the MS/MS spectra were searched against the nonredundant protein sequence database maintained at the National Center for Biotechnology Information using the Mascot program (Matrix Science, London, UK) to identify proteins. The MS/MS signal assignments were also confirmed manually.

Ni-NTA PULL-DOWN ASSAY

For Ni-NTA pull-down assays, purified MEF-E6AP was incubated with His_6-Prx proteins immobilized on Ni-NTA agarose beads (Qiagen) in 1 ml of the binding buffer [50 mM Tris-HCl (pH 7.5), 10% glycerol, 1% Triton X-100, 150 mM NaCl, 5 μM $ZnCl_2$, 1 mM Na_3VO_4, 10 mM EGTA, protease inhibitor cocktail (Complete EDTA-free)] at 4 C for 30 min. The beads were washed four times with wash buffer [50 mM Na_2HPO_4, 300 mM NaCl, 50 mM Imidazole, 0.1% Triton X-100, protease inhibitor cocktail (Complete EDTA-free)], and the pull-down complexes were separated by SDS-PAGE on 12.5% polyacrylamide gels and analyzed by immunoblotting with anti-FLAG MAb and anti-polyhistidine (His-1) MAb.

IMMUNOFLUORESCENCE MICROSCOPY

Cells were transfected with pCAG-HA-E6AP C-A and pCAG-FLAG-Prx1 using TransIT-LT1 according to the manufacturer's instructions. Transfected cells grown on collagen-coated coverslips were washed with PBS, fixed with 4% paraformaldehyde for 30 min at 4°C, and permeabilized with PBS containing 2% FCS and 0.3% Triton X-100. Cells were incubated with anti-HA mouse MAb and anti-FLAG rabbit PAb as primary antibodies, washed, and incubated with Alexa Fluor 488 goat anti-mouse IgG (Molecular Probes, Eugene, OR) and Alexa Fluor 555 goat anti-rabbit IgG (Molecular Probes) as secondary antibodies. Then, the cells were washed with PBS, mounted on glass slides, and examined with a BZ-8000 microscope (Keyence).

siRNA TRANSFECTION

HEK293T cells (3×10^5 cells in a six-well plate) were transfected with 40 pmol of either E6AP-specific small interfering RNA (siRNA; Sigma-Aldrich), or scramble negative-control siRNA duplexes (Sigma-Aldrich) using HiPerFect transfection reagent (Qiagen) following the manufacturer's instructions. The E6AP-siRNA target sequences were as follows:

siE6AP-1 (sense), 5′-GGGUCUACACCAGAUUGCUTT-3′; scramble negative control (siCont-1, sense), 5′-UUGCGGGUCUAAUCACCGATT-3′ [Shirakura et al., 2007].

IN VIVO UBIQUITYLATION ASSAY

In vivo ubiquitylation assays were performed essentially as described previously [Shirakura et al., 2007]. Where indicated, cells were treated with 25 μM MG132 (Calbiochem, La Jolla, CA) or with dimethylsulfoxide (DMSO; control) for 30 min prior to collection. FLAG-Prx1 was immunoprecipitated with anti-FLAG MAb. Immunoprecipitates were analyzed by immunoblotting, using either anti-HA PAb or anti-FLAG MAb to detect ubiquitylated Prx1.

IN VITRO UBIQUITYLATION ASSAY

In vitro ubiquitylation assays were performed essentially as described previously [Shirakura et al., 2007]. For in vitro ubiquitylation of Prx1, purified His_6-Prx1 was used as a substrate. Assays were done in 40-μl volumes containing 20 mM Tris-HCl, pH 7.6, 50 mM NaCl, 5 mM $MgCl_2$, 5 mM ATP, 8 μg of bovine ubiquitin (Sigma-Aldrich), 0.1 mM DTT, 200 ng of mouse E1, 200 ng of E2 (UbcH7), and 0.5 μg of MEF-E6AP. The reaction mixtures were incubated at 37°C for 120 min followed by immunoprecipitation with anti-Prx1 PAb. The samples were analyzed by immunoblotting with anti-Ub MAb.

IDENTIFICATION OF Prx1 AS A BINDING PARTNER FOR E6AP

To identify novel substrates for E6AP, we screened for E6AP-binding proteins using a tandem affinity purification procedure with a tandem tag (known as MEF-tag) [Ichimura et al., 2005; Shirakura et al., 2007]. Seven proteins were reproducibly detected from lysed cells transfected with MEF-E6AP C-A (Fig. 1A, lane 2), but none were recovered from lysed control cells transfected with empty vector alone (Fig. 1A, lane 1). To identify the proteins, silver-stained bands were excised from the gel, digested with Lys-C, and analyzed using a direct nanoflow liquid chromatography-MS/MS system. One of these bands, migrating at 25 kDa (Fig. 1A, lane 2, No. 7), was identified as Prx1 based on two independent MS spectra (Fig. 1B,C). To confirm the proteomic identification of Prx1, HEK293T cells were transfected with MEF-E6AP C-A plasmid or empty plasmid. The cells were lysed and immunoprecipitated with anti-Myc MAb or control IgG. Endogenous Prx1 was co-immunoprecipitated with anti-Myc MAb, suggesting that E6AP binds endogenous Prx1 (Fig. 1D, lane 4).

IN VIVO INTERACTION BETWEEN Prx1 AND E6AP

To determine whether E6AP specifically interacts with Prx1, HA-E6AP plasmid was introduced into HEK293T cells together with either FLAG-Prx1 plasmid or FLAG-Prx2 plasmid. Prx1 and Prx2 share 77.4% sequence identity at the protein level. Cells were lysed and immunoprecipitated with anti-HA MAb, anti-FLAG MAb, or

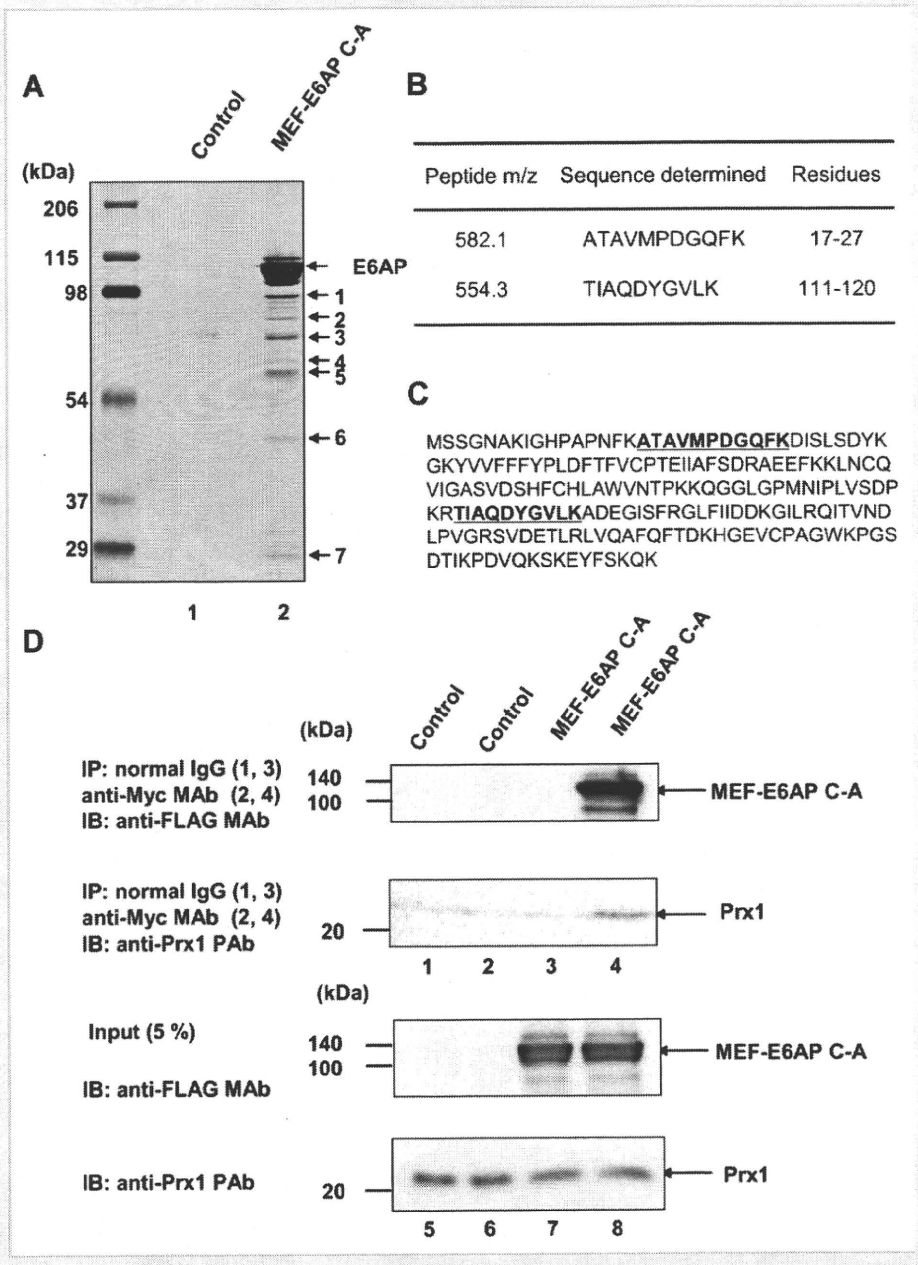

Fig. 1. Identification of Prx1 as a binding partner for E6AP. A: Prx1 interacts with E6AP in vivo. HEK293T cells were transfected with pcDNA3-MEF-E6AP C-A or empty plasmid, incubated for 48 h, and then harvested. The expressed MEF-E6AP C-A and binding proteins were recovered using the MEF purification procedure. Proteins bound to the MEF-E6AP C-A immobilized on anti-FLAG beads were dissociated with FLAG peptides, resolved by 7.5% SDS–PAGE, and visualized by silver staining. Control experiments were performed using HEK293T cells transfected with vector alone. Bound proteins were detected by SDS–PAGE and silver staining. Molecular weight markers are indicated as well as the position of p25 (No. 7), which likely corresponds to Prx1. B: Peptide masses were identified by tandem mass spectrometry. The protein was Prx1 (GenBank accession No. BC021683). C: Corresponding amino acids of Prx1 (peptides in bold print). D: HEK293T cells were co-transfected with MEF-E6AP C-A plasmid. Control experiments were performed using HEK293T cells transfected with vector alone. Cell lysates were immunoprecipitated with anti-Myc MAb or normal mouse IgG (lanes 1–4), eluted with c-Myc tag peptide. Eluates were analyzed by immunoblotting with anti-FLAG MAb or anti-Prx1 PAb. The input samples were separated by SDS–PAGE and analyzed by immunoblotting with anti-FLAG MAb or anti-Prx1 PAb (lanes 5–8). The positions of Prx1 and MEF-E6AP C-A are indicated by arrows. IB, immunoblot; IP, immunoprecipitation.

normal IgG (Fig. 2A, lanes 1–6). FLAG-Prx1 but not FLAG-Prx2 was co-immunoprecipitated with anti-HA MAb (Fig. 2A, lower panel, lanes 1 and 2). Conversely, HA-E6AP was co-immunoprecipitated with FLAG-Prx1 but not FLAG-Prx2 using anti-FLAG MAb (Fig. 2A, upper panel, lanes 3 and 4). These results suggest that E6AP specifically interacts with Prx1.

To determine whether Prx1 and E6AP co-localize in the cells, immunofluorescence microscopy analysis was performed in HEK293T cells. There was no staining without primary antibodies (data not shown). The immunofluorescence study showed that E6AP and Prx1 mainly localize in the cytoplasm and that E6AP and Prx1 co-localize in the cytoplasm (Fig. 2B, Merge).

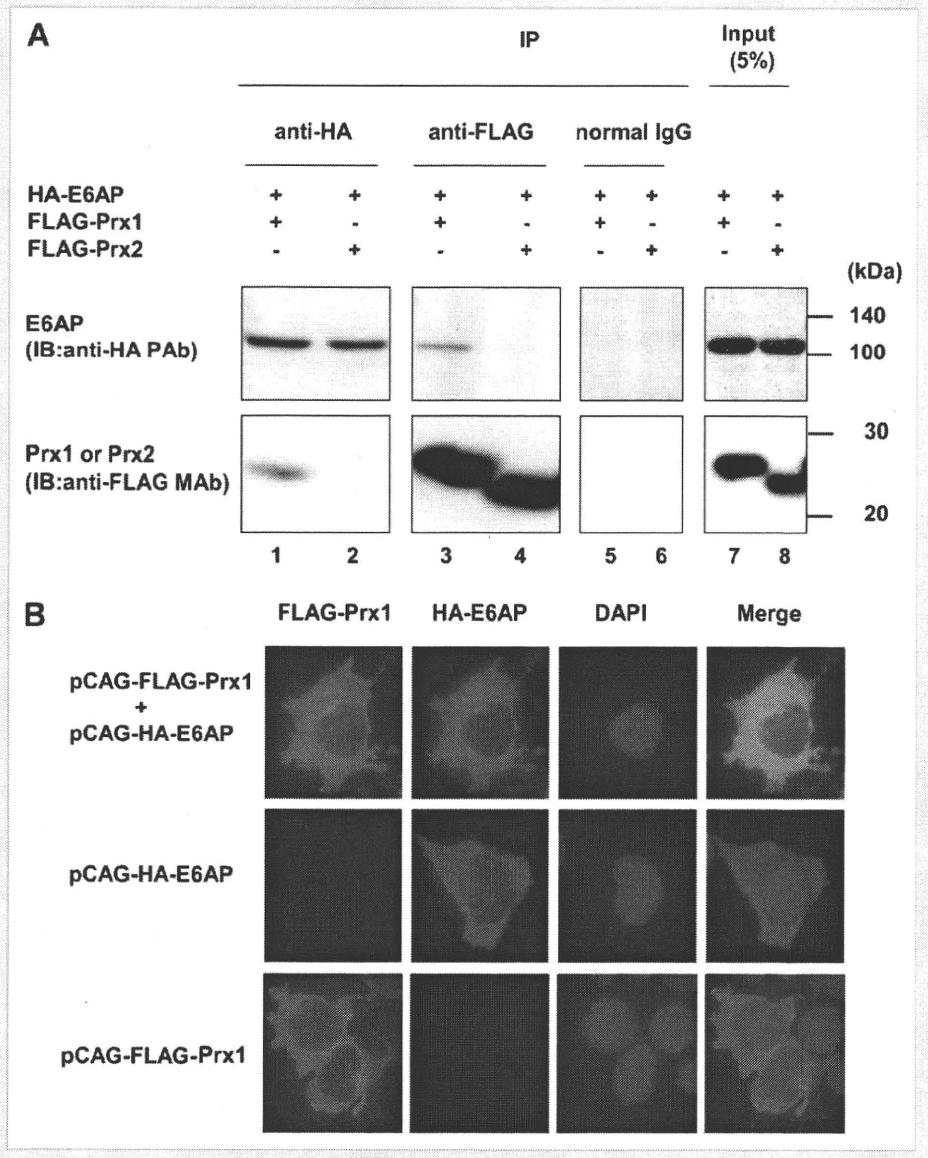

Fig. 2. In vivo interaction between Prx1 and E6AP. A: HEK293T cells were co-transfected with pCAG-HA-E6AP together with either pCAG-FLAG-Prx1 or pCAG-FLAG-Prx2. Cell lysates were immunoprecipitated with anti-HA mouse MAb, anti-FLAG mouse MAb, or normal mouse IgG and analyzed by immunoblotting with anti-HA PAb or anti-FLAG MAb. B: HEK293T cells were transfected with either HA-E6AP plasmid or FLAG-Prx1 plasmid, grown on coverslips, fixed, and processed for double-label immunofluorescence for HA-E6AP or FLAG-Prx1. All the samples were examined with a BZ-8000 microscope (Keyence).

IN VITRO INTERACTION BETWEEN Prx1 AND E6AP

To determine whether E6AP interacts with Prx1 in vitro, purified recombinant MEF-E6AP, MEF-annexin A1 expressed in insect cells using a baculovirus system and purified recombinant His_6-Prx1 and His_6-Prx2 expressed in *E. coli* were used. The His_6-tagged Prx proteins were mixed with either MEF-E6AP or MEF-annexin A1, incubated, pulled down with Ni-NTA agarose, and analyzed by immunoblotting with anti-FLAG MAb (Fig. 3, upper panel) or anti-polyhistidine MAb (Fig. 3, middle panel). MEF-annexin A1 served as a negative control to confirm that MEF-tag does not bind Prx1. MEF-E6AP was pulled down with Prx1, but not with Prx2 (Fig. 3, lanes 1 and 3), whereas annexin A1 was not pulled down with either Prx1 or Prx2 (Fig. 3, lanes 2 and 4). These results suggest that E6AP directly and specifically binds Prx1 in vitro.

E6AP DECREASES STEADY-STATE LEVELS OF Prx1 IN HEK293T CELLS

One of the characteristic features of HECT domain ubiquitin ligases is their direct association with their substrates. Thus, we hypothesized that E6AP would function as an E3 ubiquitin ligase for Prx1. We assessed the effects of E6AP on the steady-state levels of Prx1 in HEK293T cells. FLAG-Prx1 together with HA-tagged E6AP, catalytically inactive E6AP, E6AP C-A, or Nedd4 (another HECT domain ubiquitin ligase) was introduced into HEK293T cells, and the levels of Prx1 were examined by immunoblotting. The steady-state